Noname manuscript No.
(will be inserted by the editor)

Resource-Aware Adaptive Indexing for In-situ Visual Exploration and Analytics

Stavros Maroulis · Nikos Bikakis · George Papastefanatos · Panos Vassiliadis · Yannis Vassiliou

Received: date / Accepted: date

Abstract In in-situ data management scenarios, large data files which do not fit in main memory, must be efficiently handled using commodity hardware, without the overhead of a preprocessing phase or the loading of data into a database. In this work, we study the challenges posed by the visual analysis tasks in in-situ scenarios in the presence of memory constraints. We present an *indexing scheme* and *adaptive* query evaluation techniques, which enable efficient categorical based group-by and filter operations, combined with 2D *visual interactions*, such as exploration of data points on maps or scatter plots. The indexing scheme combines a *tile-based structure*, which offers efficient visual exploration over the 2D plane, with a *tree-based structure* that organizes a tile's objects based on its categorical values. The index is constructed on-the-fly, resides in main memory and is built progressively as the user explores parts of the raw file, whereas its structure and level of granularity are adjusted to the user's exploration areas and type of analysis. To handle the cases where limited resources are available, we introduce a *resource-aware index initialization mechanism* and we formulate it as an NP-hard optimization problem; we propose two efficient approximation algorithms to solve it. We conduct extensive experiments using real and synthetic datasets, and demonstrate that our approach reports interactive query response times (less than 0.04sec); and in most cases is more than $100\times$ faster and performs up to 2 orders of magnitude less I/O operations compared to existing solutions. The proposed methods are implemented as part of an open-source system for in-situ visual exploration and analytics.

Keywords Data Visualization · Visual Analytics · Progressive Indexing · In-situ Processing · Interactive Exploration

⋆ **Preprint: to appear in VLDB Journal 2022**

S. Maroulis
Nat. Tech. Univ. of Athens & ATHENA Research Center, Greece

N. Bikakis and G. Papastefanatos
ATHENA Research Center, Greece

P. Vasssiliadis
Univ. of Ioannina, Greece

Y. Vassiliou
Nat. Tech. Univ. of Athens, Greece

1 Introduction

A common task in data exploration scenarios involves *in-situ* visual data analysis, in which data scientists wish to *visually interact and analyze* large (and *dynamic*) raw data files (e.g., CSV). These users usually have limited skills in data management and *limited resources* or *commodity hardware* for use (e.g., scientist's laptop), in contrast to, e.g., a distributed environment. In such scenarios, users need to perform the analysis directly over the raw files, avoiding the tedious tasks of loading and indexing the data in a data management system. Still, they expect a very small *data-to-analysis time* and they wish to interact via a rich set of *visual exploration and analytic operations*. To this end, efficient in-situ processing of raw files is a major challenge for a large number of real-world tasks over diverse domains, such as astronomy, business intelligence, finance, telco, etc.

Example. The data scientists working in telco companies analyze network data in order to get insights regarding the network quality. Such data are commonly stored in large comma-separated data files and contain signal and latency measurements crowdsourced from IoT mobile devices, e.g., connected cars, mobile phones.[1]

Figure 1(a) presents a sample of a raw file containing five entries/objects (o_1 - o_5). Each entry *represents a signal measurement* and contains information regarding the: *geographic location* (Lat, Long), *signal strength* (Signal) and *network bandwidth* (Width), as well as network and device characteristics which take *categorical values* such as: device *brand*, *network provider*, and *network technology* (Net).

[1] For example, https://www.tutela.com

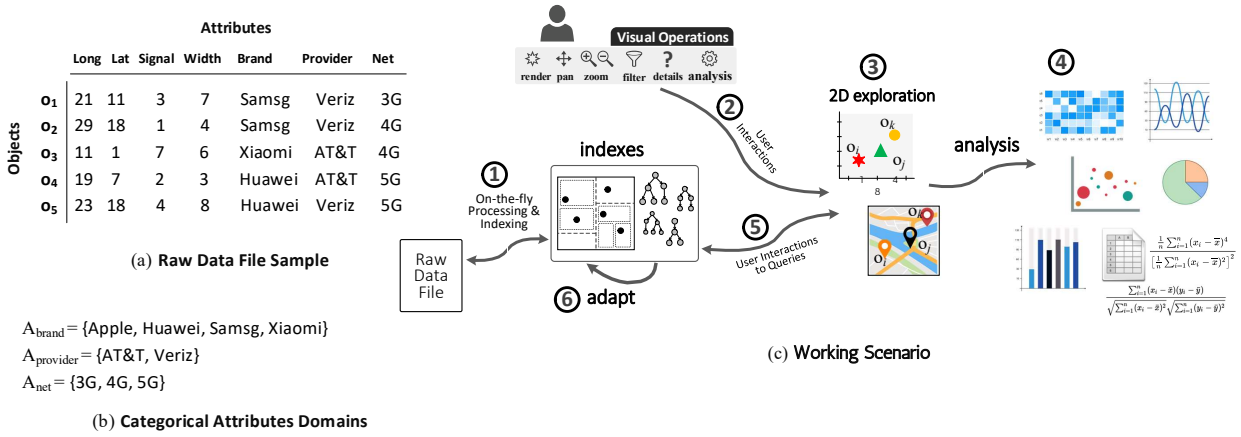

Fig. 1: (a) Raw Data File Sample (b) Categorical Attributes Domains (c) Working Scenario Overview

Assume that a data scientist wishes to *visually explore* the network data using a map. First, the user $renders$ on the map the signal measurements located in a specific geographic area, views $details$ (e.g., provider) for the points visualized, or $filters$ out the ones that refer to AT&T. Next, they may $move$ (e.g., pan left) the visualized region in order to explore a nearby area; or $zoom\text{-}in/out$ to explore a part of the region or a larger area, respectively. The scientist is also interested in *analyzing* the data considering the points in the visualized region by computing *statistics between numeric attributes*, e.g., the Pearson correlation coefficient between the signal strength and the bandwidth; or *visualize* its values using a *scatter plot*. Finally, the user may also be interested to *visually analyze data*, exploiting also the crucial information included in the *categorical attributes*; e.g., via a *heatmap* to present the average signal strength per provider and network technology, or a *bar chart* to present the average signal strength for each provider, or a *parallel coordinates* chart to present the number of measures grouped by provider, brand, and network technology.

Problem Requirements and Challenges. As demonstrated, visual exploration and analytics over raw data is essential in many real-world scenarios. Group-by analysis is required to generate well-known visualization types, such as bar charts, heatmaps, parallel coordinates, binned scatter plots, radar charts, pies, etc. Many of these charts and interactions are largely employed in common data analysis tasks, such as feature extraction, OLAP analysis, regression, and comparative analysis of spatial data [32]. Beyond the visual analytics requiring group-by operations, filter operations over categorical attributes, enables the support of *effective exploration mechanisms*, such as *faceted search*. These types of analysis and queries have been widely optimized in traditional data warehouse systems, via spatial and multidimensional indexes. However, these methods require loading the data and tuning the indexes.

In-situ techniques, on the contrary, attempt to avoid the overhead of moving, loading and indexing the data in a DBMS, and improve performance by progressively adapting an index as the user explores data. The key objective is how to offer fast user interactions without a preprocessing phase. In what follows, we highlight the requirements and technical challenges we address in this work.

In in-situ scenarios the exploratory and analysis operations are *directly evaluated over the raw file*. Using an index will enable the efficient evaluation of these operations. This index should be constructed *on-the-fly* coupled with a *small data-to-analysis time*, i.e., the time to parse and create the index should be kept small even for very large datasets. In this respect, the challenge is *how do we construct an index on-the-fly (small construction time) which can enable efficient query evaluation in interactive scenarios (fast response time)*? Additionally, since the *cost of I/O operations* has a large impact on response time, the challenge is to *design the index such that access to the file is reduced, and efficient raw file parsing is achieved*.

Next, in the cases where *commodity hardware* is used, the data in a large raw file, as well as its index, does not fit in memory. Especially, in cases where categorical attributes are involved, the memory required to index the dataset becomes prohibitive even for a small number of attributes. For example, Figure 2 shows the memory allocated for the initial "crude" version of our index, over different numbers of categorical attributes, on a relative small dataset with 100M objects (SYNTH10 dataset, Sect.8). We can observe that for 4 categorical attributes, the size of the index is 31GB, while indexing 5 attributes requires more than 64G of memory. These amounts of memory are not usually available in commodity hardware-based scenarios. The challenge here is *what part of the data do we choose to index and how do we optimize the index given a predefined memory size*?

Moreover, a challenge is related to *efficient query evaluation* over the index in exploration scenarios. The use of the information inferred by the user interactions and analysis tasks allows the improvement of the index, and the selection of metadata (e.g., statistics, aggregates) which can be used to improve the evaluation performance. Thus, the challenge here is *how do we progressively adapt the index and enrich it with metadata, such that queries are efficiently evaluated*?

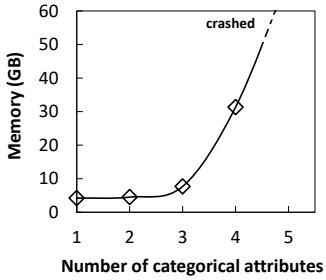

Fig. 2: Indexing Memory Requirements vs. Number of Categorical Attributes

Adaptive Indexing and In-situ Data Management. In the last decade, there are several *adaptive indexing techniques*, which aim to incrementally adjust the indexes and/or refine the physical order of data, during query processing, following the characteristics of the workload [21,16,48,19,34, 16,17,33,38]. In most cases the data has to be previously loaded/indexed in the system/memory, i.e., a preprocessing phase is considered, and such methods try to adjust the (physical) order of data, performing extensive data duplication and large memory consumption.

On the contrary, the *in-situ paradigm* has been recently adopted when analysis should be performed directly on raw data files (e.g., CSV, JSON), avoiding the overhead of fully loading and indexing the data in a DBMS. Similarly, to traditional in-database adaptive methods, in-situ techniques achieve performance by building indexes on-the-fly and progressively readjusting them as the user explores data. Works in this area have proposed techniques for progressive loading and/or indexing of raw data, for "generic" in-situ query processing (mainly range queries) [2,18,44,25,24,35], and for 2D visual operations over numeric attributes [7]. Nevertheless, in in-situ scenarios, no attention has been given for the support of: (1) exploratory aggregate queries (i.e., queries that include categorical-based group-by and filter operations) in the presence of (2) limited memory resources, such that index parameters (e.g., structure, size) are optimized to the available memory allocated for the analysis.

Our In-situ Working Scenario. Figure 1(c) presents our scenario. Assume that a user wishes to *visually explore* data using a 2D visualization technique, e.g., scatter plot, map; and *analyze* it using *visual analytics and statistics*. ① The user first selects the input file and a map as the underlying visualization layout. The file is parsed on-the-fly and an initial "crude" version of the index is constructed. ② Then, the user interacts and performs visual and analytic operations on the map ③. For example, generates visual data representations (e.g., bar charts, heatmaps), or uses statistical approaches (e.g., Pearson correlation) ④. Eventually, each user interaction and analytical operation is mapped to a query evaluated over the index ⑤, and triggers the readjustment of the index structure and the update of its contents ⑥.

Our Approach. In this work, we present an innovative *indexing scheme* (VETI) and *adaptive* query evaluation techniques in the context of in-situ visual analytics. Our methods support efficient categorical-based *group-by* and *filter* operations, combined with 2D *visual interactions*, and statistics. VETI is built on top of a *tile-based structure* which offers efficient visual exploration over the 2D plane, enhanced with a *tree-based structure* that organizes a tile's objects based on its categorical values. The index resides in main memory and is constructed on-the-fly given the first user query.

Further, we propose a query evaluation mechanism that minimizes response time by: (1) *progressively adjusting and enriching the structure and metadata kept on the index* to the user's exploration areas and type of analysis; (2) using *the index metadata for avoiding I/Os and performing memory-based computations*; and (3) accessing the the raw file *in a sequential manner*.

For reducing the memory footprint during initialization, we define a *resource-aware index initialization approach*, which we formulate as an optimization problem, referred to as SIN problem. Given the amount of available memory, the initialization approach selects the initial index characteristics (e.g., which categorical attributes to be indexed in each tile), so that the memory allocated is lower than the available amount. We show that SIN is NP-hard, even in highly restricted instances. To cope with the hardness of the SIN problem, we design two efficient approximation algorithms.

In our experiments we illustrate that our approach, in most queries, reports *interactive query response times* (*less than* 0.04sec), over large raw files (e.g., 45GB). Compared to the best existing solutions, our approach *is more than 100× faster* and performs up to 2 orders of magnitude fewer I/O operations.

The proposed methods are integrated into RawVis [29], *an open source data visualization system* for in-situ visual exploration and analytics over big raw data. The source code is available under GNU/GPL.[2] Further, [37] combines the proposed methods with real-time entity resolution techniques for the analysis of raw data files of varying quality.

Contributions. The contributions of this work are summarized as follows:

- We introduce a hybrid main-memory indexing scheme for raw data that organizes the objects based on spatial/numeric, as well as categorical attribute values.
- We formulate exploratory and analytical operations over categorical attributes, that are mapped to query operators over the underlying indexing scheme.
- We design interaction-based adaptation techniques that progressively adjust the index structure and metadata.
- We implement a resource-aware index initialization approach, based on which the index characteristics are determined w.r.t. predefined memory resources.
- We formulate the resource-aware index initialization as an optimization problem, and we show that even in highly restricted settings the problem is NP-hard. Also, we propose two approximation algorithms to solve it.

[2] The source code is available at: github.com/VisualFacts/RawVis

Table 1: Common Notation

Symbol	Description
$\mathcal{O}$, o_i	Set of objects, an object
$\mathcal{A}$, $a_{i,A}$	Set of attributes, the value of attribute A of the object o_i
A_x, A_y, $\mathcal{A}_C$	X Y Axis & Categorical attributes
$\mathcal{C}$	Ordered set of categorical attributes
Q, $\mathcal{R}$	Exploratory Query, its Results
$\mathbb{I}$, $\mathbb{I}_\mathcal{T}$	VETI index; its Tiles
h, $h.\mathcal{C}$	CET tree; its Categorical attributes
$h.N$	Number of CET nodes
$t.h$	Tree h of tile t
ρ_t, ρ_h	Tile & Tree utility
$HP_\mathcal{C}$	Attributes-based Tree Powerset, given a set $\mathcal{C}$
π_t^h, $\pi_t^h.\omega$	A Tile-Tree Assignment and its Utility
$\mathbb{I}_\Pi$, $\Omega(\mathbb{I}_\Pi)$	Index Assignments; Index Utility
$\mathcal{B}$	Initialization memory budget
$\pi_t^h.\Phi$	Memory cost estimation for assignment π_t^h
$\mathcal{H}$	Candidate tree set
$\mathbb{I}_{cost}$, $\mathbb{I}_{\mathcal{T}\,cost}$, $\mathbb{I}_{\mathcal{H}\,cost}$	Memory cost of: index $\mathbb{I}$, its tiles $\mathbb{I}_\mathcal{T}$ and its trees $\mathbb{I}_\mathcal{H}$

– We implement the presented indexing scheme and the methods in an open source visualization system.[2]
– We evaluate the performance and the effectiveness of our methods using real and synthetic datasets.

Comparison to Previous Work. Some parts of this article have been briefly presented in a preliminary version of this work [30]. Here, we significantly extend [30] as follows. (1) Regarding the *tree structure* (Sect. 3), we *formally define and analyze the complexity* of the tree operations; and introduce *new operations* related to tree adaptation. (2) Regarding the *query processing and index adaptation* (Sect. 5), we design and implement a mechanism that is based on the new expand tree operation. (3) We introduce and study a *resource-aware index initialization* mechanism (Sect. 6) and design *two approximation algorithms* for implementing it (Sect. 7). (4) In Section 8, we conduct extensive experiments with several new metrics, parameters and datasets; including experiments for the two initialization algorithms.

Compared to our previous work in the context of in-situ visual exploration [7], here, we adapt and integrate the tile-based index introduced in [7] into our indexing scheme. The rest of the concepts studied in this article are not mentioned in [7], i.e., categorical-based: (1) exploratory and analytic operations, (2) indexing scheme, (3) query processing and index adaptation; and resource-aware index initialization.

2 Exploration Model

This section presents the adopted exploration model. In this work, we extend the model presented in [7] by defining three new operations, i.e., grouping, filtering, and aggregating, over categorical attributes. The basic concepts of this work and notations are summarized in Table 1.

Raw Data File. We assume a *raw data file* $\mathcal{F}$ containing a set of *d-dimensional objects* $\mathcal{O}$. Each dimension corresponds to an *attribute* $A \in \mathcal{A}$, where A may be spatial, numeric, categorical, or textual.

Objects. Each object o_i is defined as a sorted list of d attribute values $o_i = (a_{i,1}, a_{i,2}, ..., a_{i,d})$, and associated with an *offset* f_i (a hex value) pointing to the "position" of its first attribute from the beginning of the file $\mathcal{F}$. Also, the value $a_{i,A}$ denotes the value of the attribute A for the object o_i.

Let $\mathcal{A}_C \subseteq \mathcal{A}$ denote the *categorical attributes* of the objects. Each categorical attribute A_C is represented as a finite set of values $A_C = \{v_1, v_2, ...v_n\}$, which defines the domain of the attribute, i.e., $dom(A_C)$.

User Interactions. The *exploration model* denotes a series of user interactions which are formulated as a set of operations (e.g., render, zoom). Given a raw data file, the users arbitrarily select two numeric attributes $A_x, A_y \in \mathcal{A}$, that are mapped to the X and Y axis of a 2D visualization layout (e.g., scatter plot, map). The A_x and A_y attributes are denoted as *axis attributes*, while the rest as *non-axis*.[3]

The users visualize a rectangular area $\Phi = (I_x, I_y)$, called *visualized area*, which is defined by the two intervals $I_x = [x_1, x_2]$ and $I_y = [y_1, y_2]$ over the axis attributes A_x and A_y, respectively; i.e., Φ corresponds to the 2D area $I_x \times I_y$. The visualized area contains the set of *visible objects* $\mathcal{O}_\Phi \subseteq \mathcal{O}$, for which the values of their axis attributes fall within the ranges of that area.Note that the mapping of the position (x, y) of the objects in the visualized area to their values A_x and A_y in the data is linear, e.g., spatial coordinates or any other affine mapping.

In this setting, the following *operations/interactions* are defined: (1) *render*: visualizes the objects contained in the visualized area.; (2) *move*: changes the boundaries of the visualized area, i.e., a pan operation; (3) *zoom in/out* : zooms the boundaries of the visualized area keeping the center point inside Φ fixed; (4) *filter*: excludes objects visualized in Φ, based on conditions over the non-axis attributes; (5) *detail*: presents information (e.g., attributes values) related to the non-axis attributes; (6) *group*: finds group of objects based on one or more categorical attributes, i.e., similar to the group-by operation defined in SQL; (7) *analyze*: computes aggregate or statistical functions over all objects or groups of objects in the visualized area.

These operations may be combined in a sequence; so, *a user exploration scenario is a finite sequence of operations applied by the user*.

Exploratory Query. Considering the aforementioned user operations, we define the following data-access operators, which compose the query applied to the data, referred as *exploratory query*.

Given a set of objects $\mathcal{O}$ and the axis attributes A_x and A_y, an *exploratory query* Q over $\mathcal{O}$ is defined by the tuple $\langle \mathsf{S}, \mathsf{F}, \mathsf{D}, \mathsf{G}, \mathsf{N} \rangle$, where:

[3] We assume that the users are familiar with the schema, the min/max values and the domains of the attributes in the data file; otherwise, they can have a preview of it, in terms of loading a small sample or parsing the file once.

– *Selection clause* S: defines a 2D range query (i.e., window query) specified by two intervals I_x and I_y over the axis attributes A_x and A_y, respectively. The *Selection clause* is denoted as $\mathsf{S} = (I_x, I_y)$ and its intervals are $\mathsf{S}.I_x$ and $\mathsf{S}.I_y$. This clause selects the objects $\mathcal{O}_\mathsf{S} \subseteq \mathcal{O}$, for which the values of their axis attributes fall within the respective intervals, $\mathsf{S}.I_x$ and $\mathsf{S}.I_y$. The *Selection clause is mandatory* in a query Q, while the remaining clauses are *optional*.

– *Filter clause* F: defines a set of conjunction conditions that are applied *on the non-axis attributes*. The *Filter clause* is defined as $\mathsf{F} = \{F_1, F_2, ...F_k\}$, where a condition F_i is a predicate involving an atomic unary or binary operation over object attributes and constants. The Filter clause is applied over the selected objects $\mathcal{O}_\mathsf{S}$, returning the objects $\mathcal{O}_Q$ that satisfy the F conditions.

– *Details clause* D: defines a set of non-axis attributes $\mathsf{D} = \{A_1, A_2, ...A_k\}$, for which the values of the objects O_Q, will be returned by the query.

– *Group-by clause* G: defines a set of categorical attributes $\mathsf{G} = \{A_1, A_2, ...A_k\}$ with $A_i \in \mathcal{C}$, which are used in a group-by operation. Given a set of objects O and an attributes set $\mathcal{C}$, the *group-by operation* partitions O into a set of distinct groups, denoted as $\mathcal{G}^\mathcal{C}_\mathcal{O}$, based on the different combinations of the values of the $\mathcal{C}$ attributes in the O objects. Thus, here, the *Group-by clause* G performs a group-by operation based on its attributes, over the objects satisfying the filter $\mathcal{O}_Q$, resulting in the groups $\mathcal{G}^\mathsf{G}_{\mathcal{O}_Q}$.

– *Analysis clause* L: defines two sets of algebraic aggregate functions (e.g., count, mean) [15], where each of them is applied over a set of numeric attributes, returning a single numeric value. Particularly, the *Analysis clause* defines two sets of functions: (1) L_Q that are computed over the *objects* $\mathcal{O}_Q$ *returned by the query*; and (2) L_G that are computed over *each group of objects* resulted by the group-by operations. Thus, the analysis clause is defined as: $\mathsf{L} = (L_Q, L_\mathsf{G})$. Note that, the support of algebraic aggregate functions in our model enables the computation of a large number of complex statistics, e.g., Pearson correlation, covariance.[4]

The *semantics of query execution* involves the evaluation of the different clauses of the query in the following order: (1) *Selection*; (2) *Filter*; (3) *Details*; (4) *Group-by*; (5) *Analysis*.

Mapping User Interactions to Exploratory Queries. A user interaction can be mapped to clauses of an exploratory query. Particularly, the $render$, $move$, and $zoom$ operations are implemented by the *Selection clause*; the *render* operation sets the *Selection* intervals I_x and I_y equal to the region of the visualized area, *move* sets the intervals equal to the new intervals of the shifted area and *zoom in/out* operations set the *Selection* intervals to the new coordinates of the contained/containing visualized regions, respectively. Finally, the *filter*, *details*, *group*, and *analyze* operations are implemented by the query's *Filter*, *Details*, *Group-by* and *Analysis* clauses, respectively.

Query Result. The *result* $\mathcal{R}$ *of an exploratory query* Q over $\mathcal{O}$ is defined as $\mathcal{R} = (\mathcal{V}_{x,y,\mathsf{D}}, \mathcal{V}_{L_Q}, \mathcal{V}_\mathsf{G})$, where:
(1) $\mathcal{V}_{x,y,\mathsf{D}}$ is a set of tuples corresponding to the objects $\mathcal{O}_Q$ returned by the query. For each object, its tuple contains: (a) the values of the axis attributes A_x and A_y; and (b) the values of the attributes D defined in the Details clause. Formally, $\mathcal{V}_{x,y,\mathsf{D}} = \{\langle o_i : \alpha_{i,x}, \alpha_{i,y}, \quad \alpha_{i,A_1}, ...\alpha_{i,A_k}\rangle, \forall o_i \in \mathcal{O}_Q\}$, where $\{A_1, ...A_k\} = \mathsf{D}$.

(2) $\mathcal{V}_{L_Q}$ is a list of the numeric values produced by the aggregate functions L_Q over the objects $\mathcal{O}_Q$. Formally, $\mathcal{V}_{L_Q} = \{\ell_1(\mathcal{O}_Q), \ell_2(\mathcal{O}_Q), ...\ell_k(\mathcal{O}_Q)\}, \forall \ell_i \in L_Q$.

(3) $\mathcal{V}_\mathsf{G}$ contains the results of the group-by clause. Particularly, $\mathcal{V}_\mathsf{G}$ is a set of tuples, where each tuple corresponds to a g_i group from $\mathcal{G}^\mathsf{G}_{\mathcal{O}_Q}$. Each tuple contains: (a) the values of the attributes G defined in the group-by clause; and (b) the results of the aggregate functions L_G (computed over g_i). Formally, $\mathcal{V}_\mathsf{G} = \{\langle g_i : a_{i,A_1}, ...a_{i,A_k}, \ell_1(g_i), ...\ell_z(g_i)\rangle, \forall g_i \in \mathcal{G}^\mathsf{G}_{\mathcal{O}_Q}\}$, where $\{A_1, ...A_k\} = \mathsf{G}$ and $\{\ell_1, ...\ell_z\} = L_\mathsf{G}$.

3 CET Tree: An Index for Categorical Attributes

In this section, we present a *tree structure that organizes objects based on their categorical attribute* values, named CET (Categorical Exploration Tree). CET is designed as a *lightweight*, *memory-oriented*, *trie-like* tree structure. In a nutshell, each tree level corresponds to a different categorical attribute, and edges to attribute values. Based on the tree hierarchy, each node is associated with a set of objects, that are determined based on the node path. These objects are stored in the leaf nodes.

Overall, the design of the CET tree relies on the following principles and challenges. First, considering the number of attribute-value combinations which are required for categorical indexing, a significant amount of memory is required (Fig. 2). Hence, the design of a *memory-efficient categorical structure* is a major challenge, especially in our scenario, where we consider limited available resources. To reduce the memory footprint of the tree, we implement the following techniques: (1) *Each object allocates three numeric values*: (a) two numeric values for the axis attributes; and (b) one numeric value (i.e., file offset) that offers object-based, precise "connection" between object and raw file (2) *Statistics are stored only in one tree level* (in leaves), while the hierarchical structure of CET allows the efficient computation of statistics over different levels, by performing efficient, in-memory aggregate operations. (3) *The number of tree elements is reduced* (i.e., nodes/edges) during tree construction, by considering attribute characteristics, i.e., size of the attributes' domain (see Sect. 3.1).

A second challenge is to *reduce the cost of* I/O *operations* which are crucial in such I/O-sensitive settings. Exploiting the way CET stores the objects during the initialization phase (Sect. 4.3), we are able to *access the raw file in*

[4] More than 90% and 75% of the statistics supported by SciPy and Wolfram, respectively, are defined as algebraic aggregate functions [46].

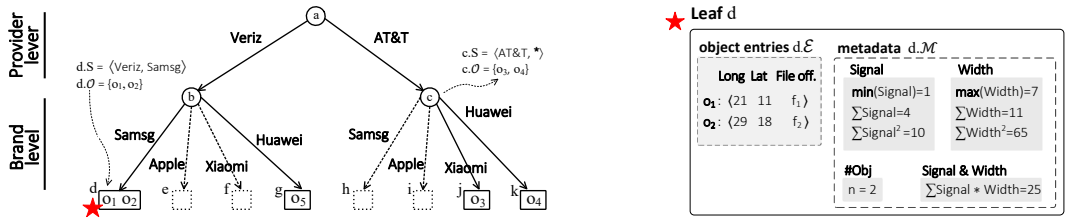

(a) **CET Tree** (b) **Contents of Leaf** d

Fig. 3: CET Tree Overview

a sequential manner. The sequential file scan increases the number of I/Os over contiguous disk blocks and improves the utilization of the look-ahead disk cache. Note that, in our experiments, *the sequential access results in about* $8\times$ *faster* I/O *operations* (more details in Sect. 5.1).

CET Structure. Given a set of objects $\mathcal{O}$ and an ordered set (list) of categorical attributes $\mathcal{C} = \{A_{C_0}, A_{C_1}, ...A_{C_k}\}$, a CET tree h organizes the objects $h.\mathcal{O}$ based on the values of the categorical attributes $h.\mathcal{C}$. The *height* of h is $|\mathcal{C}|$, so it has $|\mathcal{C}|+1$ *levels* (from 0 to $|\mathcal{C}|$), with the *leaf nodes* storing the objects.

CET follows a "level-based" organization, where *each level corresponds to a different attribute*. Specifically, based on the given order of the attributes $\mathcal{C}$, the *nodes at level* i *have edges* that correspond to a different value of the attribute $A_{C_i} \in \mathcal{C}$, i.e., $dom(A_{C_i})$.

Each node n, is *associated with a sequence of attribute values* $n.S = \langle v_0, v_1..., v_k\rangle$, that is defined by the *path from the root to node* n. The sequence contains $|\mathcal{C}|$ values, where the value v_i corresponds to a value of the attribute in level i. Specifically, for a node n at the level i, the first i^{th} values in $n.S$ are the attributes values found in the path from the root to n, while the rest $|\mathcal{C}|-i$ values are assigned with the value *any*, denoted as $*$.

Based on the sequence of values $n.S$, a node *is associated with a set of objects* $n.\mathcal{O} \in \mathcal{O}$, where its attribute values are equal to the sequence's values. As a result, the tree defines an aggregation structure, where in each node, the associated objects are the union of the objects associated with its child nodes. Note that, to reduce the memory requirements of the index, we maintain a hash table for each categorical attribute mapping its values to numeric hashes.

Object Entries. *Leaf nodes* contain references to the data objects, i.e., object entries. Note that, object entries are not included in internal nodes. For each object $o_i \in n.\mathcal{O}$, an *object entry* e_i is defined as $\langle a_{i,x}, a_{i,y}, f_i\rangle$, where $a_{i,x}, a_{i,y}$ are the values of the axis attributes and f_i the offset (a hex value) of o_i in the raw file. As $n.\mathcal{E}$ we denote the set of object entries stored in the leaf node n. In any case, an object entry has a constant size that is not affected by the object's characteristics (e.g, number of attributes), and is equal to three numeric values: the object's A_x and A_y (e.g., two double), and the object's offset from the beginning of the file, e.g., a long. The file offset f_i defines a "direct and precise" object-based connection between an object and the raw file.

Synopsis Metadata. Apart from object entries, each leaf node n is associated with a set of *synopsis metadata* $n.\mathcal{M}$, which are (numeric) values calculated by algebraic aggregate functions [15] over one or more attributes of the $n.\mathcal{E}$ objects. Combining the algebraic aggregate functions allows us to support a large number of statistics, e.g., Pearson correlation, covariance.[4] For example, we employ functions like *sum*, *mean*, *sum of squares of deltas* over the objects of a leaf. Using leaf metadata, we are able to compute the metadata of any internal node n, by aggregating the metadata of the descendant nodes of n, in a bottom-up fashion.

Example 1. [**CET Tree**] Figure 3a presents the CET index constructed for the categorical attributes $\mathcal{C} = \{A_{Provider}, A_{Brand}\}$. The dotted lines indicate parts of the tree that will not be constructed for the particular dataset.

Considering the level-based organization, the *level* 0 corresponds to the *Provider* attribute (the first attribute in $\mathcal{C}$), and *level* 1 to *Brand*. The nodes in each level have as *edges* the values of the level's corresponding attribute, e.g., edges of node a are the *Provider* values: *Provider* $= \{$Ver, AT&T$\}$.

Also, the node c has the *associated sequence values* $c.S = \langle$AT&T, $*\rangle$, where AT&T corresponds to the path of c, and the value *any* is produced by the absence of the *Brand* attribute (in the path). Further, c is *associated with the objects* $c.\mathcal{O} = \{o_3, o_4\}$ that "match" with the $c.S$ values, i.e., have as *Provider* the value *AT&T* and the value *any* for *Brand*.

Regarding the *leaf nodes*, the leaf d stores the object entries $d.\mathcal{E}$ and the metadata $d.\mathcal{M}$ for the objects $d.\mathcal{O} = \{o_1, o_2\}$ that matches its values $d.\mathcal{S} = \langle$Veriz, Samsg$\rangle$ (Fig. 3b). Here, metadata stores statistics regarding the *Signal* and the *Width* numeric attributes.

3.1 CET Operations & Analysis

Insert & Tree Construction. *Insertion* takes as input, a tree h, an object o, and an ordered set of categorical attributes $\mathcal{C} = \{A_{C_0}, A_{C_1}, ...A_{C_k}\}$ and inserts o in a leaf node based on the values $A_{\mathcal{C}_i}$ of its categorical attributes, constructing new edges and nodes for the values that do not exist in the tree. Also, the leaf metadata is updated w.r.t. the o numeric attributes. The tree *construction* is implemented via sequential $insert$ *operations* of its objects.

The *computation complexity* of the $insert$ operation is $O(|\mathcal{C}|)$, and that of *construction* considering n objects is $O(n\,|\mathcal{C}|)$.

Get Leaves/Objects Based on Filter Conditions. The *get leaves operation* returns the leaf nodes $\mathcal{L}$ of a tree h. Based on the conditions in the Filter clause F of a query, the operation constructs paths p starting from the root to the leaf nodes and returns the leaves $\mathcal{L}$ reached by all paths. The *get objects operation* returns the object entries of the leaves $\mathcal{L}$.

Regarding the *computation complexity* of the $get\ leaves$ and $get\ objects$ operations, the worst case occurs when we have to access all the leaf nodes in the tree. In that case, the complexity is $O(h.N)$ and $O(h.N + |h.\mathcal{O}|)$ respectively, where $h.N$ is the number of nodes in the tree and $h.\mathcal{O}$ its objects.

Expand Tree with New Attributes. The *expand tree* operation adds new levels in the tree and reorganizes the objects in the leaves. It is used when a query requests attributes not existing in the tree. In such cases, the values of the missing attributes retrieved from the file expand the tree (see Sect. 5). The operation takes as input the new categorical attributes $\mathcal{C}$, and a subset of leaf nodes $\mathcal{L}$ of a tree h, which should be reorganized based on $\mathcal{C}$. For each leaf node $l_i \in \mathcal{L}$, a subtree h_i having l_i as root is constructed, where h_i has one level for each attribute $A_C \in \mathcal{C}$ and leaf nodes $\mathcal{L}_{h_i}$. The objects of each leaf node l_i are organized based on $\mathcal{C}$ attributes and stored to the leaf nodes $\mathcal{L}_{h_i}$ of the generated tree h_i. Further, the metadata of the new leaf nodes $\mathcal{L}_{h_i}$ are computed.

Note that after the *expand tree* operation, the leaf nodes of the tree may appear at different levels, as only the subset of leaf nodes needed to evaluate a query are expanded with the new attributes. This way, we avoid unnecessary I/O operations by reading only the attributes for the objects included in the query. Otherwise, we would need to read the new attributes for every object in the tree in order to fully create the new attribute levels.

Regarding, the *computational complexity*, the worst case appears when the leafs $\mathcal{L}$ to expand, enclose all the tree objects $h.\mathcal{O}$. In such a case, the complexity is $O(|h.\mathcal{O}|\ |\mathcal{C}|)$.

Tree Space Complexity Analysis. Considering the CET insertion process, nodes are created based on the values of the objects being inserted in the tree. We can easily verify that the maximum number of nodes in a CET tree occurs when all possible combinations of values for its attributes appear in the objects it contains. Given the tree attributes $h.\mathcal{C} = \{A_{C_0}, A_{C_1}, ...A_{C_k}\}$, the *maximum number of nodes* $h.N$ is: $1 + |\text{dom}(A_{C_0})| + |\text{dom}(A_{C_0})| \cdot |\text{dom}(A_{C_1})| + ... + |\text{dom}(A_{C_0})| \cdot |\text{dom}(A_{C_1})| \cdot ... \cdot |\text{dom}(A_{C_k})| = 1 + \sum_{i=0}^{|h.\mathcal{C}|-1} \prod_{j=0}^{i} |dom(A_{C_j})|$. Note that the term "1" corresponds to the root node.

Considering that a leaf node is created only if it is associated with at least one object, the maximum number of leaf nodes is equal to the number of objects. Similarly, at each level of the tree the number of nodes cannot be larger than the number of objects. In what follows, we consider the *number of objects, in order to define a tighter upper bound for the total number of nodes*.

The maximum number of nodes can be determined using the following recursive formula: $\Gamma_0 = 1$ and $\Gamma_i = min(\Gamma_{i-1} \cdot |\text{dom}(A_{C_{i-1}})|, |h.\mathcal{O}|)$, with $1 \leq i \leq |h.\mathcal{C}|$. So, if we consider the number of objects is much greater than the product of the size of the attribute domains, we have that the *maximum number of nodes is*: $1 + \sum_{i=1}^{|h.\mathcal{C}|} \Gamma_i$.

Since the memory for each node is almost the same (except for the leaves where metadata is stored), here, for simplicity, we assume that all nodes allocate equal memory. Furthermore, all object entries have the same size (about four numeric values). Therefore, the *space complexity* of CET is: $O(\alpha + \alpha \sum_{i=1}^{|h.\mathcal{C}|} \Gamma_i + \beta\, |h.\mathcal{O}|)$, where α and β are the memory allocated by a node and an object entry, respectively.

Attributes Ordering vs. Tree Space. Based on the complexity analysis, we can easily verify that the number of nodes in a tree h depends on the mapping of its attributes $h.\mathcal{C}$ to the levels of the tree and the size of their domain. Assuming that the data follow a uniform distribution over the domain values of each attribute, we can reduce the number of nodes (and edges) in the tree, by placing the attributes at the levels of the tree in a top-down way based on their domain size, i.e., smaller domains are placed closer to the root. So, *constructing a tree following this attribute order, will result in lower space requirements*. In our experiments, this attribute order led to up to 10% reduction in total index memory requirements, compared to a random order (Fig. 15).

4 VETI: A Tile-Tree Adaptive Index

In this section, we present the VETI indexing scheme (Visual Exploration Tile-Tree Index), that combines the tile-based index presented in [7] and the CET tree structure. The design of VETI relies on the basic challenges posed by the in-situ exploration scenarios. First, the *index construction should entail a small overhead in the raw data-to-analysis time*. To this end, a lightweight, "crude" version of VETI is initially constructed on-the-fly, by parsing the raw file once. Moreover, the characteristics of this initial VETI version are defined by considering query and data-related factors in order to improve the performance of the initial user interactions. Second, during the exploration, the *index should support efficient exploratory and analytic operations*. Thus, based on user exploration, efficient structure adaptation and object reorganization are employed to adjust the index to user interactions. Third, considering the *limited available resources*, VETI uses lightweight tree and tile structures with predefined memory resources allocated to them (Sect. 6).

4.1 Tile Structure

Our work is built on top of a variation of the VALINOR tile-based index, referred also as *tile-structure* [7].

VALINOR is a *hierarchical tile-based* index, which is stored in memory and *organizes the data objects into hier-*

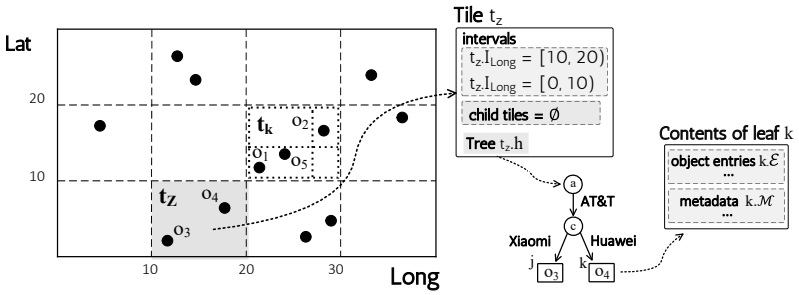

Fig. 4: VETI Index Overview

archies of non-overlapping rectangle tiles. The index's tiles are defined over the domains of the A_x and A_y attributes and a *tile* t in the grid is defined from two ranges $t.I_x$ and $t.I_y$, in the same domains, respectively. Each tile *encloses a set of objects* $t.\mathcal{O}$, when the values $a_{i,x}$ and $a_{i,y}$ of an object $o_i \in t.\mathcal{O}$ fall within the intervals, $t.I_x$ and $t.I_y$ of the tile, respectively.

$\mathcal{T}$ is the set of tiles defined in the structure. The index is initialized with an initial set of tiles (see Sect. 4.3) and progressively adjusts itself to the user interactions, by splitting the tiles visited into more fine-grained ones, thus forming a hierarchy of tiles.

In each level of the hierarchy, there are no overlaps between the tile intervals of the same level, i.e., disjoint tiles. A *non-leaf tile* t can have an arbitrary number of *child tiles*, enclosing the intervals of its children. That is, given a non-leaf tile t defined by the intervals $t.I_x = [x_1, x_2)$ and $t.I_y = [y_1, y_2)$; for each child tile t' of t, with $t'.I_x = [x'_1, x'_2)$ and $t'.I_y = [y'_1, y'_2)$, it holds that $x_1 \leq x'_1, x_2 \geq x'_2, y_1 \leq y'_1$ and $y_2 \geq y'_2$. The *Leaf tiles* correspond to tiles without children and can appear at different levels in the hierarchy.

Figure 4 presents the tile-structure of the data in Figure 1, which divides the 2D space into 4×3 equally sized disjoint tiles, and a tile t_k is further divided into 2×2 subtiles of arbitrary sizes, forming a tile hierarchy.

4.2 VETI: Combining Tiles and Trees

In this section we present the VETI index (Visual Exploration Tile-Tree Index) which combines the tile-structure with CET trees. VETI is defines as follows: given a *raw data file* $\mathcal{F}$, two *axis attributes* A_x and A_y, and a set $\mathcal{C}$ of *categorical attributes* of the objects stored in $\mathcal{F}$, the *VETI index* $\mathbb{I}$ organizes the objects stored in $\mathcal{F}$ into hierarchies of non-overlapping tiles based on its A_x, A_y values, where tiles are also associated with CET trees which organize objects based on categorical attributes from $\mathcal{C}$.

Let $\mathbb{I}_\mathcal{T}$ be the tiles of $\mathbb{I}$. Each leaf tile $t \in \mathbb{I}_\mathcal{T}$ *is associated with a CET tree* h, denoted as $t.h$. The associated tree $t.h$ of a tile t, organizes the objects $t.\mathcal{O}$ enclosed by t, based on a set of categorical attributes $\mathcal{C}' \subset \mathcal{C}$, i.e., $h.\mathcal{O} = t.\mathcal{O}$ and $h.\mathcal{C} = \mathcal{C}'$. Thus, trees of different tiles may organize their objects based on different sets of categorical attributes.

The objects $t.\mathcal{O}$ enclosed in a tile t are stored in the leaf nodes of the associated tree $t.h$ and can be accessed via a pointer to the root node of the tree $t.h$. In case the objects of a tile are not indexed based on any categorical attribute (i.e., $h.\mathcal{C} = \varnothing$), the tree h corresponds to a node (root) that stores all the object entries.

Algorithm 1. Initialization ($\mathcal{F}$, A_x, A_y, $\mathcal{C}$, Q_0, $\mathcal{B}$)

Input: $\mathcal{F}$: raw data file; A_x, A_y: axis attributes; $\mathcal{C}$: categorical attributes; Q_0: first query
Output: $\mathbb{I}$: initialized index; $\mathcal{R}_0$: result of query Q_0

1 $\mathbb{I}_\mathcal{T} \leftarrow$ IT.constructTiles($A_x, A_y, \mathcal{A}_\mathcal{C}, Q_0$) //determine the number, size & intervals of the tiles, and construct them
2 $\mathbb{I}_\Pi \leftarrow$ find tile-tree assignments //see Sect. 6
3 **foreach** $o_i \in \mathcal{F}$ **do** //read objects from file, insert them to trees & evaluate Q_0
4 *read* from $\mathcal{F}$ the values of axis and categorical $\mathcal{C}$, and the attributes required to evaluate the Q_0 Analysis clause
5 use the o_i attributes to evaluate Q_0
6 $t_i \leftarrow$ find the tile $t_i \in \mathbb{I}_\mathcal{T}$ that encloses o_i based on its axis attributes values
7 insertToTree($t_i.h, \mathcal{C}, o_i$) //insert o_i to tree $t_i.h$ (Proc. 1, Sect. 3.1)
8 **return** $\mathbb{I}$, $\mathcal{R}_0$

The VETI *index* $\mathbb{I}$ is defined by a tuple $\langle \mathbb{I}_\mathcal{T}, \mathsf{IT}, \mathsf{IH}, \mathsf{AS} \rangle$, where $\mathbb{I}_\mathcal{T}$ is the tile structure (along with the its trees) defined in the index; IT is the *tiles initialization strategy* defining the methods that determine the characteristics of the tile structure; IH is the *tree initialization strategy* defining the methods that determine the characteristics of the tree structures over the tiles; AS is the *adaptation strategy* defining the methods for reconstructing the tiles and trees based on user interaction.

The basic operations of VETI are: *initialization* (Sect. 4.3), *query evaluation* (Sect. 5), and *adaptation* (Sect. 5.2).

Example 2. [**VETI Index**] Figure 4 presents the contents of tile t_z, highlighted with grey color in the index, that contains objects o_3 and o_4. For tile t_z, the index stores its intervals $t_z.I_{Lat}$ and $t_z.I_{Long}$, its child tiles $t_z.\mathcal{C}$, and a pointer to its tree $t_z.h$, which contains nodes a, c, j, and k. Finally, the contents of the leaf node k are shown in the figure (we omit presenting the detailed object entry and the metadata).

4.3 VETI Initialization

In our approach, we do not require any preprocessing or loading phase. The index is constructed on-the-fly when the user first requests to visualize the file. During the initialization phase, the following tasks are realized. First, the char-

acteristics of the index are determined, i.e., the initial set of tiles and the structure of each tree assigned to each tile are defined; then, the file is parsed and the index is populated; finally, the first user query is evaluated.

Algorithm 1 outlines the initialization phase. It takes as input, the raw file $\mathcal{F}$, the axis and categorical attributes A_x, A_y and $\mathcal{A}_\mathcal{C}$, and the first exploratory query Q_0; and returns the initialized index $\mathbb{I}$ and the results $\mathcal{R}_0$ of the Q_0.

Initially, the tile structure characteristics are determined (i.e., number, size and intervals of the tiles) and the tiles $\mathbb{I}_\mathcal{T}$ are constructed (*line* 1). Next, based on the constructed tile structure, the assignments $\mathbb{I}_\Pi$ of trees to tiles $\mathbb{I}_\mathcal{T}$ are determined (*line* 2). Details about the assignment selection methods are presented in Section 6.

In the next part (*loop in line* 3), the algorithm scans the file $\mathcal{F}$ and reads, for each object o_i, the values of the axis attributes $a_{i,x}$, $a_{i,y}$, the categorical attributes, and the attributes which are required to evaluate the Analysis clause of Q_0 (*line* 4). Next, the tile t_i that encloses o_i is found (*line* 6), and the insertToTree method (Procedure 1), inserts o_i into the tree $t_i.h$ (*line* 7). During the insertion, the object entry is constructed, the tree metadata are updated, and new parts (i.e., nodes, edges) of the tree may be constructed.

Tile Structure Initialization. The constructTiles method is defined by the tile initialization strategy IT, and determines the tile structure characteristics, e.g., number, size and intervals of the tiles. These characteristics can be defined via numerous approaches (for more details see [39]). For instance, they can be either given explicitly by the user, e.g., in a map the user defines a default scale of coordinates for the initial visualization; determined by the visualization setting, considering certain characteristics (e.g., visualization type, screen size/resolution), previous sessions, task, user preferences [39,22,3,43]; or computed based on techniques that consider data characteristics in order to divide the data space into tiles of equal size [6].

In this work, we use a *query-driven initialization policy* for initializing the tiles, adapted from [7], which considers: (1) the user exploration entry point, i.e., the position of the first user query in the 2D space; (2) the window size of the first query; and (3) the locality-based behavior of the exploration scenarios, i.e., users are more likely to explore nearby regions of their initial entry point [49,23,43,3,47, 11]. In nutshell, the query-driven tile initialization defines a tile structure that is more fine-grained (i.e., having a larger number of smaller tiles) in the area around the initial query, whereas the size of tiles becomes larger as their distance from the initial query increase.

In more details, first, the tile initialization method considers an initial set of tiles T_0 with each tile having a fixed size $l_{0x} \times l_{0y}$ (details on the selection of these parameters are described in [7]). Then, it computes for each tile $t \in T_0$ an initialization split factor SF. The latter determines the number of equally-sized subtiles that this tile t will be split into. For example, if $SF_{Q0}(t) = 4$, the tile t will be split into 4 equally-sized subtiles, with size of $(l_{0x}/2) \times (l_{0y}/2)$. For computing the split factor SF, we consider a bivariate normal distribution around the initial query position, which assigns larger numbers to tiles close to the initial query's center, i.e., tiles are split into more subtiles around the initial user query.

Increasing the number (i.e., decreasing the size) of tiles near the first query, increases the probability that subsequent queries in this neighborhood overlap with fully-contained tiles, which in turn reduce the number of I/O's. As an *I/O operation* we denote the file access in order to read an object (i.e., all attributes values), or some of its attribute values. So, the number of I/O operations corresponds to the number of rows from which we read attribute values. More details about query evaluation are presented in the next section.

Discussion. Note that, beyond CET trees, we also studied alternative structures for indexing categorical attributes in VETI. Specifically, we considered the use of bitmap structures which are effective for indexing low cardinality attributes and are highly compressible. In brief, in a VETI variation we implemented, we combined the tile structure with a set of bitmap structures instead of CET trees. In this variation, based on the objects $t.\mathcal{O}$ of a tile t, a bitmap structure is constructed for each distinct value of every categorical attribute in $t.C$. As in our approach, apart from the object entries, each bitmap is also associated with a set of metadata pertaining to its objects indexed in it. Note that, several other bitmap-based variations were studied, however due to lack of space their descriptions are omitted.

In our experiments, as it was expected, the bitmap variations requires, in general, less memory than the VETI with CET trees. This is not only the result of the use of the highly compressible bitmaps, but also because the bitmap variations maintain metadata for single categorical attribute values and not for different combinations. On the other hand, the query evaluation performance is significantly lower. The limited metadata stored in the bitmap variations cannot be utilized to avoid I/Os for queries that involve two or more categorical attributes. As a result, VETI is in most queries more than 2-3$\times$ faster and requires less than the half I/O operations compared to the bitmap implementations.

5 Query Processing & Index Adaptation

This section describes the query processing methods of our approach. Figure 5 outlines the workflow, whose steps are described in the following example[5]. More details on the query evaluation over the index are given in Section 5.1 and on index adaptation in Section 5.2.

Example 3. [***Query Processing & Index Adaptation***] As input we have the initialized index, an exploratory query and a raw file. Considering the objects in Figure 1, we assume an exploratory query Q with the following clauses

[5] Note that, since several details are omitted, the order of the steps may be different compared to the following paragraphs, where the process is presented in detail. Also, in the implementation, several of these steps are performed in parallel.

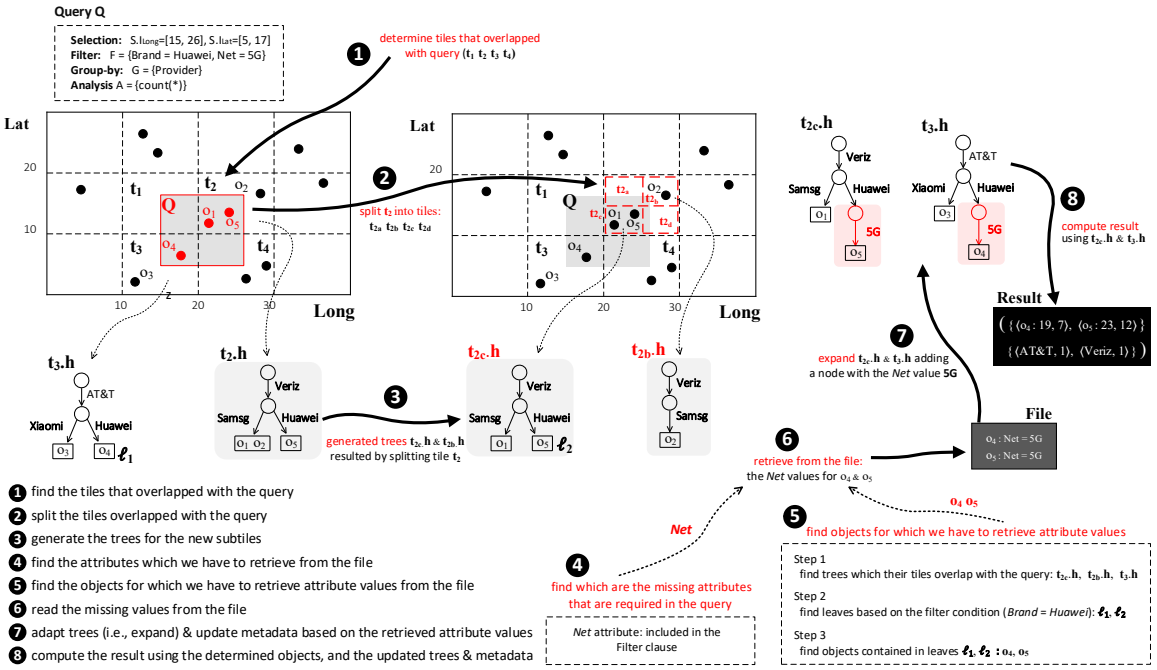

Fig. 5: Query Processing & Index Adaptation Example

(left upper corner in Fig. 5) : (1) *Selection clause*: S with S.I_{Long}=[15, 26] & S.I_{Lat}=[5, 17]; (2) *Filter clause*: F = $\{Brand = \text{Huawei}, Net = \text{5G}\}$; and (3) *Group-by clause*: G = $\{Provider\}$; and (4) *Analysis clause*: L = $\{count(*)\}$.

Further, we assume that the index is initialized and every tile has a tree with the attributes *Provider* and *Brand*. Additionally, the tree leaves contain aggregate metadata for the *Signal* attribute. The query processing and index adaptation are depicted in Figure 5.

❶ To evaluate query Q we first *find the leaf tiles that spatially overlap* (i.e., partially or fully-contained) with its Selection clause, i.e., t_1, t_2, t_3, t_4. ❷ Next, we *check if the overlapping tiles need to be split*, in such case, the tiles are split into smaller subtiles. The tile splitting may be performed based on different methods, such as: equally or arbitrary-sized splitting. In each splitting step, the process considers criteria related to I/O cost in order to decide whether to perform a split or not (more details at Sect. 5.2). In our example, we assume that t_2 is split into four equal disjoint subtiles: t_{2_a}, t_{2_b}, t_{2_c}, t_{2_d}. ❸ Then, the objects are reassigned to the new subtiles and their *trees are generated*; here, the trees $t_{2_c}.h$ and $t_{2_b}.h$ of the new subtiles t_{2_b} and t_{2_c}.

❹ We, then, find *the attributes of the query which are not contained in the index*, and for which their values have to be retrieved from the file. In our example, the query's Filter clause includes conditions over the *Brand* and *Net* attributes, i.e., *Brand* = Huawei, *Net* = 5G. Also, the Group-by clause contains the *Provider* attribute. Since the index was initialized to include the categorical attributes *Brand* and *Provider*, values for the *Net* attribute are not available in the index.

❺ We *determine the objects for which we have to read the NET attributes from the file*. For that, considering the tiles that overlapped with the query (t_{2_a}, t_{2_b}, t_{2_c}, t_{2_d}, t_3, t_4), we *identify the trees of these tiles* ($t_{2_b}.h$, $t_{2_c}.h$ and $t_3.h$.) and we traverse each tree for identifying their *leaves which evaluate to the query's condition Brand* = Huawei. These leaves are ℓ_1 and ℓ_2 from the trees $t_{2_c}.h$ and $t_3.h$, which contain the objects o_4 and o_5. ❻ For these objects, we *read the file* and retrieve the *Net* attribute values.

❼ Based on the values retrieved from the file, *trees are adapted/expanded* (e.g., create new nodes/edges, reorganize leaf objects) in order to include the new attribute and *update the metadata*. Here, using the retrieved *Net* values of o_4 and o_5, the trees $t_{2_c}.h$ and $t_3.h$ are *expanded* to include the new categorical attribute *NET* (see *expand* operation, Sect. 3.1).

❽ Finally, query Q *is evaluated* on the objects o_4 and o_5 for the condition *Net* = 5G, and on the tree metadata for the *Group by* and *Analysis* clauses. In our example, the *count* function is calculated by the number of objects in each leaf node. The result consists of: the tuples of the selected objects o_4 and o_5 and their axis attributes ($\{\langle o_4 : 19, 7\rangle, \langle o_5 : 23, 12\rangle\}$); and the tuples that form the result of the *Group by* and *Analysis* clause ($\{\langle AT\&T, 1\rangle, \langle Veriz, 1\rangle\}$).

5.1 Query Processing

The main query processing is presented in Algorithm 2. The algorithm also includes the index adaptation phases, which are analyzed in the next section. The algorithm takes as input, the initialized index $\mathbb{I}$, an exploratory query Q and the raw file $\mathcal{F}$. Next we provide details on the implementation of each step presented in the previous example.

Find and Adapt Query's Overlapped Tiles & Trees. Once the index has been initialized, the algorithm finds the leaf

Algorithm 2. Query Processing ($\mathbb{I}$, Q, $\mathcal{F}$)

Input: $\mathbb{I}$: index (initialized); $Q\langle \mathsf{S}, \mathsf{F}, \mathsf{D}, \mathsf{G}, \mathsf{L}\rangle$: query; $\mathcal{F}$: raw data file
Variables: $\mathcal{T}_\mathsf{S}$: leaf tiles that overlap with the Selection clause, i.e., 2D area; $\mathcal{T}_a$: tiles resulted from adaptation; $\mathcal{L}$: tree leaf nodes selected by the Query; $\mathcal{W}(\langle l, \mathcal{V}\rangle)$: set of tuples $\langle l, \mathcal{V}\rangle$, where $\mathcal{V}$ are objects' attributes, and l its leaf
Parameters: AS: adaptation strategy;
Output: $\mathcal{R}$: result of query Q

1 $\mathcal{L} \leftarrow \varnothing$
2 $\mathcal{T}_\mathsf{S} \leftarrow$ getLeafTilesOverlappedWithQuery $(\mathbb{I}_\mathcal{T}, \mathsf{S})$
3 **foreach** $t_s \in \mathcal{T}_\mathsf{S}$ **do**
4 $\quad \mathcal{T}_a \leftarrow$ AS.adaptTileAndTree (t_s, Q) //see Sect. 5.2
5 $\quad \forall t_a \in \mathcal{T}_a : \ \mathcal{L} \leftarrow \mathcal{L} \bigcup$ getLeavesBasedOnFilter $(t_a.h, \mathsf{F})$ //Procedure 2 (Sect. 3.1)
6 $\mathcal{W}(\langle l, \mathcal{V}\rangle) \leftarrow$ getLeavesRequiringFileAccess $(\mathcal{L}, Q)$ //set of tuples, where $\mathcal{V}$ are the attributes of a leaf l whose their values need to be retrieved from the file
7 **if** $\mathcal{W} \neq \varnothing$ **then** //values are missing — read from file
8 $\quad$ *read from file* the values of attributes $\mathcal{V}$ for the objects of leaf l, $\forall\langle l, \mathcal{V}\rangle \in \mathcal{W}$
9 $\quad$ expandTree $(l, \mathcal{V})$ $\forall\langle l, \mathcal{V}\rangle \in \mathcal{W}$ //update tree based on retrieved attributes; i.e., expand tree's leaf l with its missing attributes $\mathcal{V}$ (Sect. 3.1)
10 $\quad$ updateLeafMetadata (l) $\forall l \in \mathcal{W}$
11 $\mathcal{R} \leftarrow$ *evaluate* Q using the objects and the metadata of leaves $\mathcal{L}$
12 **return** $\mathcal{R}$

tiles $\mathcal{T}_\mathsf{S}$ that overlap with the 2D area defined in the query's Selection clause S (*line* 2). The function getLeafTiles OverlappedWithQuery determines the overlapping tiles at the highest-level, and then traverses the tile hierarchy to find the set of overlapping leaf tiles $\mathcal{T}_\mathsf{S}$.

Next, based on the adaptation strategy AS, the adaptTileAndTree procedure (*line* 4), performs the tile splitting and reorganizes the trees (constructing new or modifying existing) that are included in the tiles $\mathcal{T}_a$ created by the splitting process (more details in Sect. 5.2). Finally, considering any conditions over categorical attributes that are defined in the Filter clause, getLeavesBasedOnFilter retrieves the leaf nodes $\mathcal{L}$ of the $\mathcal{T}_a$ trees (*line* 5).

Determine the Objects that Require File Access. After identifying the tiles overlapping with the query and the corresponding leaves, we determine the objects for which we have to access the raw file in order to answer the query.

Procedure getLeavesRequiringFileAccess $(\mathcal{L}, Q)$ (*line* 6), first, considers the spatial relation between the 2D area specified in a Select clause and the tiles it overlaps. Specifically, a *tile* t that overlaps a query Q can be *partially-contained* or *fully-contained* in Q. So, the procedure for each leaf node in $\mathcal{L}$, first checks if the tile it belongs to, is partially or fully-contained in the query Q. In the case that a leaf belongs to a *partially-contained tile*, the leaf metadata can not be used, since only a subset of a (leaf's) objects could be selected by the query. Hence, we need to find the objects of the leaf that are contained in the query; then, for these objects, we retrieve from the file the attributes required to compute the metadata and evaluate the Analysis clause of the query.

Apparently, in the case that a leaf belongs to a *fully-contained tile*, we do not need to traverse its objects in order to find the ones that are included in the window and the tile's metadata can be used without the need to access the file. In fully-contained tiles, file access is needed only when the query refers to attributes for which *information is not stored in the index*, e.g., *Net* attribute in the query example.

Based on the aforementioned, the procedure getLeavesRequiringFileAccess identifies the attributes, whose values have to be retrieved from the file. Finally, it returns a list $\mathcal{W}$ of tuples $\langle l, \mathcal{V}\rangle$, where $\mathcal{V}$ are the attributes that must be retrieved for the objects included in the leaf l.

Read Objects' Attributes from File. To *reduce the cost of reading the missing attributes from file (line 8)*, we exploit the way the object entries are stored in the leaves in order to access the file in a sequential manner. During the initialization of the index, we append the object entries into the leaf nodes of the CET trees as the file is parsed. As a result, object entries in every leaf node are stored sorted based on their file offset. When accessing the file, we read the objects from the leaves following a k*-way merge* based on their file offset. Thus, we are able to *access the raw file in a sequential manner*. The sequential file scan increases the number of I/O operation over continuous disk blocks and improves the utilization of the look-ahead disk cache. Note that, in our experiments, *the sequential access results in about* $8\times$ *faster* I/O *operations* compared to accessing the file by reading objects on a "leaf basis", i.e., read the objects of leaf l_i, then read the objects of tile l_k, etc.

Adapt Trees and Update Metadata based on the Attributes Read from File. Next, based on the attributes for which values are read from the file, the trees (of fully-contained tiles) are adapted/enriched to include the retrieved attributes. Particularly, the expandTree procedure (Sect. 3.1) adapts/enriches the trees by including the retrieved attributes and reorganizes the objects (*line* 9). As already discussed in Section 3.1, the expandTree procedure expands the trees only for the objects that it needs to read from the file to evaluate the query. This partial tree expansion adapts the trees with new attributes without performing unnecessary I/O operations. Then, the function updateLeafMetadata computes and updates the metadata using the values retrieved from the file (*line* 10).

Evaluate Query. Finally, we evaluate query Q using the objects and metadata of the leaf nodes $\mathcal{L}$ (*line* 11). Here we use the attribute values retrieved from the file to check the filter conditions that do not involve categorical attributes. Also, we need to check the objects belonging to trees missing some of the categorical attributes included in the Filter clause. Finally, the Group-by and Analysis clauses are evaluated using: (1) existing metadata of the fully-contained tiles, if their corresponding CET trees include all the categorical attributes of the query; (2) for all other cases, the values retrieved from the file.

5.2 Incremental Index Adaptation

VETI employs an *incremental index adaptation* model that attempts to adapt the index structure to the query workflow of the user exploration. Each query may result in splitting

the tiles overlapping the Selection clause into smaller subtiles. *Tile splitting increases the likelihood that a tile included in the area that the user exploration focuses on, will be fully-contained in a future query* and the use of metadata in fully-contained tiles will reduce the number of file accesses, improving the query performance. For that reason, splitting is performed as a first step of the query evaluation process, such that we compute metadata for the new subtiles and then evaluate the query over a more fine-grained index. Specifically, it is performed after function getLeafTiles OverlappedWithQuery has determined the leaf tiles that overlap with the Selection clause (*line* 2).

Procedure adaptTileAndTree (*line* 4) is responsible for the incremental adaptation. It takes as input a tile t and a query Q and returns a set of subtiles $\mathcal{T}_a$ if t needs to be split.

To split, or not to split? During query processing, we examine each tile that overlaps with the query if it needs to be split. To determine if a tile t requires (further) splitting, we define a model that estimates the *expected splitting gain* in terms of I/O cost, for evaluating a (future) query Q, in case of splitting t. If the expected splitting gain for a tile, exceeds a given splitting threshold, a split is performed. A further analysis of the splitting model is presented in [7].

In our implementation, the I/O cost is formulated by the selectivity of Q over t, where selectivity is computed by the number of objects in t and the filter conditions defined in Q.

Tile Splitting. After the tile splitting, the adaptTileAndTree (*line* 4) procedure returns a set of subtiles $\mathcal{T}_a$. Each one of the children contains a tree with the same set of categorical attributes as their parent tile. The objects contained in the leaf nodes of the parent tile's tree are reorganized in the leaf nodes of the new trees according to their values for the axis attributes, as well as the categorical attributes.

In our implementation for VETI, we employ a quad-tree like splitting approach in which a tile is split into 4 equal subtiles. However, more sophisticated methods can be used to split a tile, e.g., query based splitting methods [7].

Reorganize Trees in Splitted Tiles. As discussed in Section 3.1, the order of the attributes in a tree affects its size (number of nodes/edges). Hence, during splitting, the attributes of the trees that are generated in the new subtiles, are sorted so that the attributes with smaller domain sizes are placed closer to the root. For this, we consider the distinct values of the categorical attributes within the bounds of the parent tile t. Then, we reorganize the objects of t into the trees of the children $\mathcal{T}_a$.

To reorganize the objects, we perform Depth-first search in the tree $t.h$ to iterate over all of its leaf nodes. Based on the path of every leaf node from the root, we can determine the values of its categorical attributes. Then, for each object entry of a leaf node, we find the subtile that encloses it and we insert it into its tree (using the $insert$ operation).

Adaptation Computation Complexity. The overall computational cost of tile splitting, consists of the cost of splitting the tile t, constructing $\mathcal{T}_a$, and reorganizing the objects $t.\mathcal{O}$ in $\mathcal{T}_a$ trees. First, we have to determine the intervals of $\mathcal{T}_a$, and define the subtiles as child tiles of t, i.e., initialize the child pointers. These can be performed in constant time $O(1)$. Then, we perform Depth-first search (DFS) in the tile's tree h, and reinsert its objects into the trees of the subtiles. The cost of DFS is $O(h.N)$, where $h.N$ is the number of nodes in the tree, and the cost of the $insert$ operation is $O(|h.\mathcal{C}|)$. So, the overall cost is $O(h.N + |t.\mathcal{O}|\,|h.\mathcal{C}|)$.

6 Resource-aware Index Initialization

In this section, we present the initialization of the CET trees and their assignment to tiles. Recall from Figure 2, that more than 64GB is required for VETI to create full trees from five categorical attributes. Our goal here is to determine the structures of the trees (the categorical attributes that will be placed as levels in the tree) and assign them to tiles based on the "utility" of each tree. The latter depends on the utility of the categorical attributes it contains; we consider that an attribute has a higher utility score when its inclusion in the tile's tree is expected to improve *the performance in the user exploration scenario*.

We define the *ReSource-aware INdex Initialization* (SIN) problem and formulate and solve it as an optimization problem of assigning trees to tiles based on the utility score. In what follows, we first provide some preliminaries and then define the SIN problem.

6.1 Preliminaries

Tile Utility. Let a tile t, the *tile utility* $\rho_t \in [0, 1]$ formulates the possibility that a future exploratory query will overlap with t. For the distribution of ρ_t, we follow the approach in [7]. Based on the locality-based characteristics of 2D exploration scenarios, users are more likely to explore nearby regions of their initial exploration entry point [49,23,43,3, 47,11]. Thus, given an initial query Q_0, the next queries are more likely to overlap with tiles near Q_0 and the value of ρ_t is larger in tiles near Q_0. Particularly, in [7] the probability that a query overlaps with a tile t is modeled considering a bivariate normal distribution based on the distance of the tiles from the center of Q_0.

Attribute Score & Tree Utility. We assume that *each categorical attribute c has a score $c.S \in [0, 1]$*, that represents the probability that a future query will request this attribute. We define the attribute score based on the "repetitive calculation of statistics" that appears in exploration scenarios [46], i.e., we assume that the attributes requested by the initial query Q_0, are more likely to be requested by next user interactions. Using the attributes scores, the tree utility is defined as follows.

Given a tree h, the *tree utility* $\rho_h \in [0, 1]$ formulates the possibility that an exploratory query requests information stored in the tree. Without loss of generality, we define the *tree utility* ρ_h as the normalized sum of the scores of the tree attributes $h.\mathcal{C}$:

$$\rho_h = \frac{\sum\limits_{\forall c \in h.\mathcal{C}} c.S}{\sum\limits_{\forall c \in \mathcal{C}} c.S} \quad (1)$$

Example 4. [***Running Example***] Consider a VETI index with six *tiles* (t_1- t_6); three categorical attributes *Provider* (P), *Brand* (B) and *Net* (N), with domain size 2, 4, and 3, respectively; and a *query* Q_0 that includes a *Group-by clause* on attribute P, and a *Filter clause* on attribute B. We assume that Q_0 overlaps with t_1 and based on the other tiles' position, the *tile utilities* are: $\rho_{t_1} = 0.6$, $\rho_{t_2} = 0.1$, $\rho_{t_3} = 0.1$, $\rho_{t_4} = 0.1$, $\rho_{t_5} = 0.05$, and $\rho_{t_6} = 0.05$.

Regarding the *categorical attribute scores*, the attributes P and B are included in Q_0 and assigned with a score 0.8, whereas N has score 0.1. Additionally, assume the trees: $h_{P,B}.\mathcal{C} = \{P, B\}$, and $h_{P,N}.\mathcal{C} = \{P, N\}$. The tree $h_{P,B}$ that includes both attributes of Q_0 will have a larger utility than $h_{P,N}$ which includes only one of them. Based on the Eq. 1 the *tree utilities* are $\rho_{h_{P,B}} = 0.96$ and $\rho_{h_{P,N}} = 0.82$.

Tile-Tree Assignment. A *tile-tree assignment* (or simply *assignment*) π_t^h, assigns *a tree h to a tile t*. So, given a tile t and a tree x an assignment π_t^x defines that $t_i.h = x$.

Tile-Tree Assignment Utility Each *tile-tree assignment π_t^h is associated with a utility* $\pi_t^h.\omega \in [0, 1]$, which formulates the possibility that a query is going to request information from the tile t involving the attributes $h.\mathcal{C}$ of its tree. Intuitively, the utility formulates the "effectiveness of the information" contained by a tile-tree assignment during query evaluation. The *tile-tree assignment utility* is defined as the joint probability of the *tile utility* ρ_t and the *tree utility* ρ_h:

$$\pi_t^h.\omega = \rho_t \cdot \rho_h \quad (2)$$

Attributes-based Tree Powerset. Given a set of categorical attributes $\mathcal{C}$, the *attributes-based tree powerset* $HP_{\mathcal{C}}$, contains the trees generated by considering all possible subsets of $\mathcal{C}$. That is $2^{|\mathcal{C}|}$ trees, containing also the tree with no attributes, i.e., empty tree.

Index Assignments. Given a VETI index $\mathbb{I}$, its tiles $\mathbb{I}_{\mathcal{T}}$, and the categorical attributes $\mathcal{C}$; the *index assignment set* $\mathbb{I}_{\Pi}$ contains all the tile-tree assignments defined in the index tiles $\mathbb{I}_{\mathcal{T}}$, i.e., $\mathbb{I}_{\Pi} = \{\pi_t^h : t \in \mathbb{I}_{\mathcal{T}} \text{ and } h \in HP_{\mathcal{C}}\}$.

Example 5. [***Assignments***] Consider the index of the Example 4. The *attributes-based tree powerset* for the attributes P, B, N is: $HP_{\{P,B,N\}} = \{h_{P,B,N}, h_{P,B}, h_{P,N}, h_{B,N}, h_P, h_B, h_N, h_{empty}\}$. An assignment over $\mathbb{I}$ can include any tree from this set, e.g., the *index assignment set* $\mathbb{I}_{\Pi} = \{\pi_{t_1}^{h_{P,B,N}}, \pi_{t_2}^{h_N}, \pi_{t_3}^{h_{P,B,N}}\}$

Table 2: SIN Example: Tile-tree Assignment Utilities

	Tree						
Tile	$h_{P,B,N}$ (33)	$h_{P,B}$ (9)	$h_{P,N}$ (11)	$h_{B,N}$ (16)	h_P (2)	h_B (4)	h_N (3)
t_1 (0.6)	0.60	0.56	0.32	0.32	0.28	0.28	0.04
t_2 (0.1)	0.10	0.09	0.05	0.05	0.05	0.05	0.01
t_3 (0.1)	0.10	0.09	0.05	0.05	0.05	0.05	0.01
t_4 (0.1)	0.10	0.09	0.05	0.05	0.05	0.05	0.01
t_5 (0.05)	0.05	0.05	0.03	0.03	0.02	0.02	0.00
t_6 (0.05)	0.05	0.05	0.03	0.03	0.02	0.02	0.00

assigns the tree $h_{P,B,N}$ to tiles t_1, t_3; h_N to t_2, and no assignments (i.e., empty tree) are made for tiles t_4, t_5, t_6.

Index Utility. The *index utility* Ω of the entire index $\mathbb{I}$ is the sum of the utilities of all tile-tree assignments $\mathbb{I}_{\Pi}$ made in the index, which is defined as:

$$\Omega(\mathbb{I}_{\Pi}) = \sum_{\forall \pi_t^h \in \mathbb{I}_{\Pi}} \pi_t^h.\omega \quad (3)$$

Index Initialization Cost. The *index initialization cost* $\mathbb{I}_{cost}$ denotes the resources (e.g., memory, time) that are required for the VETI initialization. Here, as *resource* we only refer to memory. Specifically, the index initialization cost denotes the memory allocated by the index structures (i.e., tiles, trees, metadata), and does not include the memory required by the object entries that allocate a constant amount of memory; each object allocates three numeric values (Sect. 3).

This cost includes: (1) the $\mathbb{I}_{\mathcal{T}_{cost}}$ of constructing the tiles $\mathbb{I}_{\mathcal{T}}$, which is mainly the memory allocated for the tile intervals, pointers to subtiles, and the pointers connecting tiles and trees; and (2) the $\mathbb{I}_{\mathcal{H}_{cost}}$ of constructing the CET trees of the tiles (i.e., the trees defined in the tile-tree assignments), which is the memory allocated for the tree nodes, edges and metadata stored in the leaf nodes. Thus, the VETI *initialization cost* is: $\mathbb{I}_{cost} = \mathbb{I}_{\mathcal{T}_{cost}} + \mathbb{I}_{\mathcal{H}_{cost}}$.

Index Initialization Budget. We assume an *index initialization budget* $\mathcal{B}$, which is the upper bound of the index initialization cost $\mathbb{I}_{cost}$. In other words, $\mathcal{B}$ denotes the maximum memory size that can be allocated during the initialization.

6.2 Problem Definition & Analysis

The *ReSource-aware INdex Initialization* problem is defined as follows.

Resource-aware Index Initialization Problem (SIN). Given a set of objects $\mathcal{O}$ with categorical attributes $\mathcal{C}$, a set of tiles $\mathbb{I}_{\mathcal{T}}$, and a budget $\mathcal{B}$; our goal is to find the index tile-tree assignments set $\mathbb{I}_{\Pi}^*$ of a VETI index $\mathbb{I}$ with tiles $\mathbb{I}_{\mathcal{T}}$, such that the index utility Ω is maximized and the index initialization cost $\mathbb{I}_{cost}$ is lower than the budget $\mathcal{B}$.

$$\Omega(\mathbb{I}_{\Pi}^*) = \arg\max \Omega(\mathbb{I}_{\Pi}) \quad \text{and} \quad \mathbb{I}_{cost} \leq \mathcal{B}$$

Example 6. [***SIN Problem***] Based on Example 4, we assume the six tiles ($t_1 - t_6$) and the attributes P, B, N. Table 2 presents the tile-tree assignment utilities (Eq. 2) for all the possible assignments over the tiles, the tiles utilities (in parenthesis), and the cost of every possible tree (in parenthesis). Here, the cost of the trees is expressed in number of tree nodes, and we assume that all combinations of attribute values appear in the data (for space complexity see Sect. 3.1). For example, based on the domain of the attributes P, B, N (Example 4) the tree $h_{P,B,N}$ has cost (number of nodes) equal to 33. Also, the assignment $\pi_{t_1}^{h_{P,B,N}}$ that assigns tree $h_{P,B,N}$ to tile t_1 has utility $\pi_{t_1}^{h_{P,B,N}}.\omega = 0.6$.

In order to solve SIN from Table 2 we have to determine the tile-tree assignments that maximize the total index utility and keeps the assignment cost lower than the available budget. Let 50 be the budget available for the tree structures, expressed in total number of tree nodes in the index. We can verify, that the index assignment set $\mathbb{I}_{\Pi} = \{\pi_{t_1}^{h_{P,B}}, \pi_{t_2}^{h_{P,B}}, \pi_{t_3}^{h_{P,B}}, \pi_{t_4}^{h_{P,B}}, \pi_{t_5}^{h_{P,B}}, \pi_{t_6}^{h_P}\}$ corresponds to a solution of SIN. Particularly, these assignments result in a total index utility $\Omega(\mathbb{I}_{\Pi})$ equal to 0.9 (which is the largest), and the cost $\mathbb{I}_{\mathcal{H}_{cost}}$ of its trees is 47.

Theorem 1. The SIN problem is NP-hard.

PROOF SKETCH. We reduce our problem to the 0-1 Knapsack Problem (KP), which is known to be NP-hard and which states that there is a bin with a capacity, and a set of items. Each item has a weight and a profit. The goal is to find a set of items that maximizes the sum of the profits and the sum of weights is lower than the bin's capacity.

We consider a *restricted instance* of SIN, where: (1) the index contains one tile; (2) the tile utility is equal to one; (3) each attribute has a construction cost (i.e., the memory overhead when it is included in a tree); and the tree cost is the sum of its attributes' costs.

We reduce SIN to KP via the following *associations*: (1) bin to tile; (2) bin capacity to memory budget minus the cost for constructing the tiles; (3) item to categorical attribute; (4) item profit to attribute score; and (5) item weight to attribute construction cost. We can verify that, the index utility in SIN corresponds to the total profit in KP; and the budget constraint to the capacity constraint, respectively. ■

7 SIN Algorithms

In this section, we propose two approximation algorithms in order to solve the SIN problem.

The optimal solution of the SIN problem would be to examine the utility scores of all possible tree assignments from the powerset $HP_{\mathcal{C}}$ to the tiles $\mathbb{I}_{\mathcal{T}}$, and select the set of assignments that maximizes the total utility and its index initialization cost is lower than the memory budget. In the worst case we have to examine $O(2^{|\mathcal{C}||\mathbb{I}_{\mathcal{T}}|})$ tile-tree assignments (including empty trees).

In what follows we present two approximation algorithms to solve the SIN problem. The algorithms is based on two concepts: they examine a subset of *candidate trees* from the powerset $HP_{\mathcal{C}}$, in order to prune the space of the possible assignments; and they estimate a memory cost for the trees in order to handle the budget constraint. In what follows, we define the basic concepts.

7.1 Preliminaries

Candidate Trees. The *candidate trees* is a subset of the $HP_{\mathcal{C}}$ set, that contains $|\mathcal{C}|$ trees with "promising" categorical attributes, i.e., the ones that are expected to increase the index utility. To determine the promising attributes, we sort the attributes $\mathcal{C}$ in a descending order, by a *gain score* $gain(c)$, that combines: (1) the *attribute score* $c.S$ (Sect. 6.1); and (2) the *attribute memory cost*. The latter formulates the memory overhead, when c is included in a tree. Since the memory cost of a tree depends on the number of distinct values of its attributes, we consider the domain size $|dom(c)|$ to quantify each attribute's memory cost. We define the *gain score* of an attribute c as: $gain(c) = \frac{c.S}{|dom(c)|}$.

Given a gain-ordered list L_g of attributes $\mathcal{C}$, the *candidate tree set* $\mathcal{H}$, is defined by $|\mathcal{C}|$ trees, where each tree $h_i \in \mathcal{H}$ contains the first $(i+1)^{th}$ attributes of L_g. Therefore, the *candidate tree set* is $\mathcal{H} = \{h_0, ..h_{|\mathcal{C}|-1}\}$, with $h_i.\mathcal{C} = \{L_g[0], ...L_g[i]\}$. The *computational cost* for generating the candidate tree set, employing a linearithmic sorting algorithm (e.g., mergesort) is $O(|\mathcal{C}|\ log|\mathcal{C}|)$.

The candidate tree set can be characterized as a *small number of trees*, where each of them has *different memory cost* (i.e., number of attributes), while containing *as many "promising" attributes as possible*. The proposed algorithms consider only the candidate trees in the assignment selection process. This way, we reduce the $2^{|\mathcal{C}|}$ possible trees we have to examine to $|\mathcal{C}|$, significantly pruning the search space of the SIN problem.

Example 7. [***Candidate Trees***] From Example 4 we have the *attribute scores:* $A_P.S = 0.8$, $A_B.S = 0.8$, and $A_N.S = 0.1$. Also, we have the the following *domain sizes*: $|dom(P)| = 2$, $|dom(B)| = 4$, and $|dom(N)| = 3$. Hence, the *attributes gain scores* are $gain(P) = 0.8/2$, $gain(B) = 0.8/4$, and $gain(N) = 0.1/3$. Based on the gain scores, the sorted list of attributes is $L_g = \{P, B, N\}$. Thus, the *candidate trees* are $\mathcal{H} = \{h_P, h_{P,B}, h_{P,B,N}\}$, where $h_P.\mathcal{C} = \{P\}$, $h_{P,B}.\mathcal{C} = \{P, B\}$, and $h_{P,B,N}.\mathcal{C} = \{P, B, N\}$.

Tile-Tree Assignment Cost Estimation. The tile-tree assignment cost denotes the memory allocated by the assignment's tree. Recall from Section 3 that, a tree is populated during the initial file parsing, with the distinct values that appear in the categorical attributes of the data objects it contains. Therefore, the actual tree size is not known a priori, and should be estimated during index initialization.

Algorithm 3. GRD ($\mathbb{I}_{\mathcal{T}}, \mathcal{A}_{\mathcal{C}}, \mathcal{B}_{\Pi}$)

Input: $\mathbb{I}_{\mathcal{T}}$: initialized tiles; $\mathcal{A}_{\mathcal{C}}$: categorical attributes; $\mathcal{B}_{\Pi}$: memory budget for trees
Output: $\mathbb{I}_{\Pi}$: selected tile-tree assignments list
Variables: W_{π}: assignments list max-heap; $Cost_{\Pi}$: selected assignments appr. cost

1 $\mathcal{H} \leftarrow$ generateCandTrees($\mathcal{A}_{\mathcal{C}}$) //generate candidate trees
2 **foreach** $(t, h) \in \mathbb{I}_{\mathcal{T}} \times \mathcal{H}$ **do** //generate assignments & compute utilities
3 compute $\pi_t^h.\omega$ and $\pi_t^h.\Phi$ //assignment utility (Eq.2) & appr. cost (Sect.6.1)
4 $\pi_t^h.score \leftarrow$ assgnScore($\pi_t^h.\omega$, $\pi_t^h.\Phi$) //compute assignment score w.r.t. assignment's utility $\pi_t^h.\omega$ and appr. cost $\pi_t^h.\Phi$
5 push π_t^h to W_{π} //initialize assignments max-heap
6 $Cost_{\Pi} \leftarrow 0$;
7 **while** $Cost_{\Pi} < \mathcal{B}_{\Pi}$ and $W_{\pi} \neq \varnothing$ **do** //select assignments
8 $\pi_{t_\gamma}^{h_\gamma} \leftarrow pop(W_{\pi})$ //select (and remove) the top assignment
9 insert $\pi_{t_\gamma}^{h_\gamma}$ into $\mathbb{I}_{\Pi}$ //the selected assignment is inserted into assignments list
10 $Cost_{\Pi} \leftarrow Cost_{\Pi} + \pi_{t_\gamma}^{h_\gamma}.\Phi$
11 **return** $\mathbb{I}_{\Pi}$

As estimation we consider the worst case (i.e., the maximum memory a tree can require), that is defined by the maximum number of nodes the tree can have (see *Tree space complexity analysis* in Sect. 3.1). Let $nodes_{max}(\nu, \mathcal{C})$ denote the maximum number of nodes of a tree that contains $\mathcal{C}$ attributes and ν objects.

Assuming a uniform distribution of objects over the tiles, the estimated number of nodes per tile is $\nu_t = |\mathcal{O}_{DS}| \cdot \frac{areaSize(t)}{areaSize(DS)}$, where $areaSize(DS)$ and $areaSize(t)$ are the sizes of the 2D areas defined by the dataset objects (i.e., grid area size $|dom(A_x)| \cdot |dom(A_y)|$), and a tile t, respectively; and $|\mathcal{O}_{DS}|$ is the number of objects in the dataset. So, the *maximum cost estimation* for an assignment π_t^h is $\pi_t^h.\Phi = nodes_{max}(\nu_t, \mathcal{C}) \cdot n_{cost}$, where n_{cost} is the memory allocated by a single node.[6]

Eviction Mechanism. During the assignment selection, there are cases where the memory allocated for the trees during the file parsing is larger than the estimated. Also, during user exploration, the memory allocated for storing new trees, tiles, and statistics, may exceed the amount available.

In such cases, we adopt a simple eviction policy, where some trees are selected to be evicted based on their tile utility value ρ_t. So, the tile with the lowest utility is selected, and its tree is removed from memory. When a tree gets evicted, its structure (i.e., nodes, edges, and metadata) is erased and its object entries are reassigned to a single root node attached to the corresponding tile.

7.2 Greedy Tile-Tree Assignments Algorithm (GRD)

Here we present a greedy algorithm (GRD) that finds the tile-tree assignments. The basic idea is that we first compute a utility score for each candidate assignment between a tree and a tile. All assignments are sorted in descending order based on their score. The algorithm selects the top assignments and aggregates their cost up to the one for which the total estimated cost is lower than the budget.

Algorithm Description. Algorithm 3 presents the pseudocode of GRD. GRD first generates the candidate tree set $\mathcal{H}$, using the generateCandTrees function (*line* 1). For each tile $t \in \mathbb{I}_{\mathcal{T}}$ and candidate tree $h \in \mathcal{H}$ (*loop in line* 2), the algorithm defines the assignment π_t^h, computes the assignment's utility $\pi_t^h.\omega$, and the assignment's estimated cost $\pi_t^t.\Phi$ (*line* 3).

Using these metrics, the function assgnScore computes the assignment score $\pi_t^h.score$, which increases w.r.t. assignment utility and decreases w.r.t. assignment cost (*line* 4). Formally, let x_1 and x_2 assignments utilities, and y_1 and y_2 assignments costs, then:
assgnScore$(x_1, y_1) \geq$ assgnScore$(x_2, y_1) \Leftrightarrow x_1 \geq x_2$, and
assgnScore$(x_1, y_1) \geq$ assgnScore$(x_1, y_2) \Leftrightarrow y_1 \leq y_2$.

Next, the assignment is inserted (using the $push$ operation) into a max-heap W_{π} that sorts the assignments in descending order based on $\pi_t^h.score$ (*line* 5).

Next, GRD selects assignments as far as the total estimated cost Π_{cost} for the selected assignments is lower than the memory budget $\mathcal{B}_{\Pi}$, and the heap is not empty (*loop in line* 7). The assignment $\pi_{t_\gamma}^{h_\gamma}$ which has the largest score is selected and removed from the heap via the pop operation (*line* 8). Next, $\pi_{t_\gamma}^{h_\gamma}$ is inserted into the selected assignments list $\mathbb{I}_{\Pi}$ (*line* 9) and the estimated cost is updated (*line* 10). Obviously, if an assignment for a tile t is selected, the rest of the assignments referring to t are not examined.

Example 8. [***GRD Algorithm***] In this example, we assume that the estimated cost $\pi_t^t.\Phi$ of an assignment (Sect. 7) is equal to the cost presented in Table 2. Also, the assignment score is equal to assignment utility presented in Table 2. Finally, as in Example 6, we assume a budget of 50.

Initially, the algorithm computes the assignment scores for each tile (t_1 - t_6) and the candidate trees $\mathcal{H} = \{h_P, h_{P,B}, h_{P,B,N}\}$. Then, based on their score, the tile-tree assignments are sorted in descending order.

Then, the algorithm selects the assignment with the largest score, i.e., $\pi_{t_1}^{h_{P,B,N}}$. After this selection the assignments referring to tile t_1 are omitted. During the selection process, in each selection the algorithm ensures that the cost for the selected assignments does not exceed the available budget.

In the end, the algorithm selects the assignments $\mathbb{I}_{\Pi} = \{\pi_{t_1}^{h_{P,B,N}}, \pi_{t_2}^{h_{P,B}}, \pi_{t_3}^{h_P}, \pi_{t_4}^{h_P}, \pi_{t_5}^{h_P}, \pi_{t_6}^{h_P}\}$, in this order. The index utility $\Omega(\mathbb{I}_{\Pi})$ for these assignments is 0.835 and the estimated construction cost 50.

Complexity Analysis. The candidate trees require $O(|\mathcal{C}|\ log|\mathcal{C}|)$ (*line* 1). The first loop (*lines* 2-5) is executed $|\mathbb{I}_{\mathcal{T}}|\ |\mathcal{C}|$ times. The score (*lines* 4 & 5) is computed in constant time $O(1)$, and the $push$ operation (*line* 5) is performed in $O(1)$, assuming that W_{π} is a Fibonacci max-heap. Thus, the loop cost is $O(|\mathbb{I}_{\mathcal{T}}|\ |\mathcal{C}|)$. The second loop (*lines* 7-10), in the worst case is executed $|\mathbb{I}_{\mathcal{T}}|\ |\mathcal{C}|$ times. The insertion

[6] Recall that, the memory for each node is (almost) the same, with the exception of the leaf nodes where metadata is stored. For simplicity, we assume that all nodes have equal memory size.

Algorithm 4. BINN ($\mathbb{I}_{\mathcal{T}}, \mathcal{A}_{\mathcal{C}}, \mathcal{B}_{\Pi}$)

Input: $\mathbb{I}_{\mathcal{T}}$: initialized tiles; $\mathcal{A}_{\mathcal{C}}$: categorical attributes; $\mathcal{B}_{\Pi}$: memory budget for trees
Parameters: BS: binning strategy; AI: assignments initialization strategy; TS: tree selection strategy
Output: $\mathbb{I}_{\Pi}$: selected tile-tree assignments list
Variables: $L_{\mathcal{I}}$: list of bins' intervals; $L_{\mathcal{T}}$: list of tile sets per bin; $L_{\mathcal{H}}$: list of selected trees for the tiles of each bin; $\mathcal{H}$: candidate trees; $Cost_{\Pi}$: selected assignments appr. cost

1 $L_{\mathcal{I}} \leftarrow$ BS.determineBinsIntervalsOverTilesProb($\mathbb{I}_{\mathcal{T}}$) //intervals are defined over tiles' probabilities ρ_t; $L_{\mathcal{I}}[i]$ is the interval of i^{th} bin; intervals $L_{\mathcal{I}}$ are in ascending order
2 $L_{\mathcal{T}} \leftarrow$ group tiles $\mathbb{I}_{\mathcal{T}}$ into bins based on intervals $L_{\mathcal{I}}$ // $L_{\mathcal{T}}[i]$ is the set of tiles contained in the bin i that is defined by the interval $L_{\mathcal{I}}[i]$
3 $\mathcal{H} \leftarrow$ generateCandTrees($\mathcal{A}_{\mathcal{C}}$) //generate candidate trees
4 $L_{\mathcal{H}}[i] \leftarrow \varnothing \quad 0 \leq i \leq |L_{\mathcal{I}}| - 1$ //selected trees list; $\mathcal{L}_{\mathcal{H}}[i]$ contains the tree selected for the tiles $L_{\mathcal{T}}[i]$ of the bin i
5 $Cost_{\Pi} \leftarrow 0$ //selected assignments appr. cost
6 **if** AI is $defined$ **then** //an assignments initialization strategy has been defined
7 **for** $i \leftarrow 0$ **to** $|L_{\mathcal{I}}| - 1$ **do** //assignments initialization – assign initial trees to bins
8 $L_{\mathcal{H}}[i] \leftarrow$ AI.selectInitialTreeForBin($i, L_{\mathcal{H}}, L_{\mathcal{T}}, \mathcal{H}, \mathcal{B}_{\Pi}, Cost_{\Pi}$)
9 $Cost_{\Pi} \leftarrow Cost_{\Pi} +$ assignmentsCostInBin($L_{\mathcal{T}}[i], L_{\mathcal{H}}[i]$)
10 **if** $Cost_{\Pi} \geq \mathcal{B}_{\Pi}$ **then break**
11 **for** $i \leftarrow 0$ **to** $|L_{\mathcal{I}}| - 1$ **do** //find trees for bins (and possibly update/replace the inital)
12 $L_{\mathcal{H}}[i] \leftarrow$ TS.selectTreeForBin($i, L_{\mathcal{H}}, L_{\mathcal{T}}, \mathcal{H}, \mathcal{B}_{\Pi}, Cost_{\Pi}$)
13 $Cost_{\Pi} \leftarrow Cost_{\Pi} +$ assignmentsCostInBin($L_{\mathcal{T}}[i], L_{\mathcal{H}}[i]$)
14 **if** $Cost_{\Pi} \geq \mathcal{B}_{\Pi}$ **then break**
15 **for** $i \leftarrow 0$ **to** $|L_{\mathcal{I}}| - 1$ **do** //generate assignments
16 $\forall t \in L_{\mathcal{T}}[i]:$ insert $\pi_t^{L_{\mathcal{H}}[i]}$ into $\mathbb{I}_{\Pi}$
17 **return** $\mathbb{I}_{\Pi}$

in a linked list is $O(1)$, and the amortized cost of each *pop* operation is $O(log(|\mathbb{I}_{\mathcal{T}}|\ |\mathcal{C}|))$. Thus, the (amortized) complexity for the second loop is: $O(|\mathbb{I}_{\mathcal{T}}|\ |\mathcal{C}|\ \ (log(|\mathbb{I}_{\mathcal{T}}|\ |\mathcal{C}|) + 1)) = O(|\mathbb{I}_{\mathcal{T}}||\mathcal{C}|log(|\mathbb{I}_{\mathcal{T}}||\mathcal{C}|))$. Therefore, the overall (amortized) complexity for the GRD algorithm is: $O(|\mathcal{C}|\ log|\mathcal{C}| + |\mathbb{I}_{\mathcal{T}}|\ |\mathcal{C}| + |\mathbb{I}_{\mathcal{T}}|\ |\mathcal{C}|\ log(|\mathbb{I}_{\mathcal{T}}|\ |\mathcal{C}|)) = O(|\mathbb{I}_{\mathcal{T}}|\ |\mathcal{C}|\ log(|\mathbb{I}_{\mathcal{T}}|\ |\mathcal{C}|))$.

7.3 Binning-Based Tile-Tree Assignment Algorithm (BINN)

In this section, we propose the *Binning-Based Tile-Tree Assignment* algorithm (BINN). The basic idea of BINN is that the tiles are organized into bins, and the same candidate tree is assigned to every tile belonging to the same bin.

BINN Basic Characteristics. (1) The *bin-based tile organization* phase, in which the tiles are grouped into bins. The tree assignments are defined at bin-level and, thus, are not "strictly" affected by tile-specific factors, which in many cases may not be accurately estimated, such as the tile probability and the tile-tree assignment cost. (2) The *assignment initialization phase*, which defines "default" assignments for (some) tiles. These assignments may be updated/replaced during the assignment selection process. Hence, this phase enables the algorithm to "impose" assignments to a set of tiles and/or "influence" the assignment selections that follow. For example, BINN may assign a tree with one attribute to the tiles with probability larger than a threshold, or to the top-k tiles. (3) The *assignment selection phase*, which traverses and assigns a tree to each bin, by considering the selected and the default assignments in the rest of the bins.

BINN vs. GRD. BINN tackles a shortcoming of the GRD algorithm. Particularly, GRD allocates most of the budget assigning trees with all categorical attributes included (Fig. 10). As a result, trees are assigned to a smaller number of tiles. On the other hand, the bin-based approach adopted by the BINN algorithm leads to a more "balanced" allocation of the budget, with more tiles being assigned with trees having fewer categorical attributes. As demonstrated (Sect.8), in many cases, the small number of trees assigned by GRD compared to BINN has great impact in algorithms performance. In general, BINN is more than 1.5× faster and perform the half I/Os compared to GRD. To also remark that, in several cases BINN is more than 100× faster (Fig. 13).

Algorithm Description. Algorithm 4 presents the pseudocode. Using the binning strategy BS, the algorithm determines the bins as a list of probability intervals $L_{\mathcal{I}}$, which are defined based on the probabilities of the input tiles $\mathbb{I}_{\mathcal{T}}$ (*line* 1). Then, tiles are inserted into the list $L_{\mathcal{T}}$ (*line* 2) and the candidate trees $\mathcal{H}$ are generated (*line* 3).

In the next step, if an assignment initialization strategy AI has been defined (*line* 6), the algorithm performs the assignments initialization phase. For each bin i (*loop in line* 7), function selectInitialTreeForBin determines the default tree $L_{\mathcal{H}}[i]$ of the i^{th} bin (*line* 8). Next, function assignmentsCostInBin computes the cost of this assignment, considering the assigned tree $L_{\mathcal{H}}[i]$ for the tiles $L_{\mathcal{T}}[i]$ of bin i (*line* 9).

In the assignment selection phase (*loop in line* 11) and based on the tree selection strategy TS, the selectTreeForBin assigns one of the candidate trees $\mathcal{H}$ to bin i (*line* 12). In cases where an initialization phase is performed, the default tree may be replaced by the selected ones. Finally, it generates the tree assignments $\pi_t^{L_{\mathcal{H}}[i]}$ (*loop in line* 15) based on the tree $L_{\mathcal{H}}[i]$ selected for each bin i.

Strategies Details. Without loss of generality, in our experiments, the binning strategy BS uses equal frequency binning to define the bin intervals. The selectInitialTreeForBin (*line* 8) and selectTreeForBin (*line* 12) functions may consider several factors such as: the already assigned trees $L_{\mathcal{H}}$ (assigned either during initialization, or during selection), the currently available budget ($\mathcal{B}_{\Pi} - Cost_{\Pi}$), the distribution of tile probabilities, etc. In our implementation, we define a simple selectTreeForBin function, which assigns to each bin the candidate tree $\mathcal{H}[k]$ with the larger number of attributes, such that the cost of already selected and initialized assignments is lower than the budget. So, the function selectTreeForBin for a bin i selects:

$$\mathcal{H}[k] \quad \text{s.t.} \quad \arg\max \mathcal{H}[k] \quad \text{and}$$
$$Cost_{\Pi} + \text{assignmentsCostInBin}(L_{\mathcal{T}}[i], \mathcal{H}[k]) < \mathcal{B}_{\Pi}.$$

Example 9. [***BINN Algorithm***] As in the previous example, we assume that the estimated assignment cost and score are equal to the cost and the utility presented in Table 2,

and the budget is equal to 50. We adopt an equal frequency binning strategy to define the bin intervals (e.g., we consider two bins), and as selectTreeForBin we use the method described above. Based on the tile utilities shown (in parenthesis) in Table 2, the following bins of tiles are defined: $L_{\mathcal{T}} = \{\{t_1, t_2, t_3\}, \{t_4, t_5, t_6\}\}$.

First, we consider the case where no assignment initialization strategy AI is used. Then, the list of trees selected for the bins is: $L_{\mathcal{H}} = \{h_{P,B}, h_P\}$, i.e., $h_{P,B}$ selected for the first bin. Finally, the tile-tree assignment set selected by the algorithm is: $\mathbb{I}_{\Pi} = \{\pi_{t_1}^{h_{P,B}}, \pi_{t_2}^{h_{P,B}}, \pi_{t_3}^{h_{P,B}}, \pi_{t_4}^{h_P}, \pi_{t_5}^{h_P}, \pi_{t_6}^{h_P}\}$, which results in a total index utility $\Omega(\mathbb{I}_{\Pi})$ equal to 0.85 and total estimated cost 33. Considering an AI strategy which pre-assigns a default $h_{P,B}$ to every tile, the final assignments become $\mathbb{I}_{\Pi} = \{\pi_{t_1}^{h_{P,B}}, \pi_{t_2}^{h_{P,B}}, \pi_{t_3}^{h_{P,B}}, \pi_{t_4}^{h_{P,B}}, \pi_{t_5}^{h_{P,B}}, \pi_{t_6}^{h_P}\}$, which result in total index utility $\Omega(\mathbb{I}_{\Pi}) = 0.9$ and total estimated cost 47.

Complexity Analysis. To determine the intervals of the bins (*line* 1) adopting a simple binning method (e.g., equal width/ frequency binning) can be performed by sorting (e.g., merge-sort) and traversing once the tiles list. That is performed in $O(|\mathbb{I}_{\mathcal{T}}|\ log|\mathbb{I}_{\mathcal{T}}| + |\mathbb{I}_{\mathcal{T}}|)$. Then, in the worst case, organizing the tiles into bins (*line* 2) are performed in $O(|\mathbb{I}_{\mathcal{T}}|)$. The candidate trees require $O(|\mathcal{C}|\ log\ |\mathcal{C}|)$ (*line* 3).

We can easily verify that a large number of "rational" selectInitialTreeForBin (*line* 8) and selectTreeForBin (*line* 12) functions, cost $O(|L_{\mathcal{T}}[i]||\mathcal{C}|)$ in order to select a tree for bin i. In each selection, these functions examine the candidate trees CT, and in the same time compute the different costs. Since, in such functions the cost is computed during the selection, the function assignmentsCostInBin is omitted. Note that, the same complexities also hold in the functions used in our implementation. Thus, in the worst case, the *loop in line 7* costs $O(|\mathbb{I}_{\mathcal{T}}||\mathcal{C}|)$; the same also holds for the *loop in line 11*. In the last loop in the worst case, the insert operation (*line* 16) is executed $|\mathbb{I}_{\mathcal{T}}|$ times. Thus, the cost of the insertions in the linked list is $O(|\mathbb{I}_{\mathcal{T}}|)$.

Therefore, in the the worst case the complexity of BINN is the sum of the aforementioned steps: $O(|\mathbb{I}_{\mathcal{T}}|\ log|\mathbb{I}_{\mathcal{T}}| + |\mathbb{I}_{\mathcal{T}}| + |\mathbb{I}_{\mathcal{T}}| + |\mathcal{C}|\ log|\mathcal{C}| + |\mathbb{I}_{\mathcal{T}}||\mathcal{C}| + |\mathbb{I}_{\mathcal{T}}||\mathcal{C}| + |\mathbb{I}_{\mathcal{T}}|) = O(|\mathbb{I}_{\mathcal{T}}|\ log|\mathbb{I}_{\mathcal{T}}| + |\mathcal{C}|\ log|\mathcal{C}| + |\mathbb{I}_{\mathcal{T}}|\ |\mathcal{C}|)$.

8 Experimental Analysis

The objective of our evaluation is to assess the performance of our approach in terms of time and number of I/Os. We evaluate different VETI variations and several competitors over two real and two synthetic datasets. Next, we outline the key findings of our study.

Results Highlights. (1) *Performance Overview*: In most queries, VETI exhibits *response time less than* 0.04sec, over large raw files (e.g., 45GB). Regarding the best of the examined systems, in most queries VETI *is up to 100× faster* and performs up to *2 orders* of magnitude fewer I/O operations.
(2) *Data Characteristics*: All VETI variations report (sub-)linear performance w.r.t. the number of objects and categorical attributes, as well as the domain size.
(3) *VETI Variations*: Regarding the VETI variations, both VETI-BINN and VETI-GRD outperform the naive VETI-RND. VETI-BINN is more than 1.5× faster and requires about half the I/O operations compared to VETI-GRD. VETI-BINN performs even better when the user moves further away from the initial query and/or when the initialization budget is small.
(4) *Initialization Phase*: In the initialization phase, VETI-BINN is on average 8× faster than MySQL, 1.2× faster than PRAW, and slightly slower than VALINOR.

8.1 Experimental Setup

Datasets & Queries. In our experiments we have used two *real datasets*, the *NYC Yellow Taxi Trip Records* (TAXI) and *a telecommunication network quality dataset* (NET); and two synthetic ones (SYNTH10 / 50).[7]

Queries Template. Each query contains: (1) a *Select* clause defined over the axis-attributes; (2) a *Group-by* clause on a categorical attribute; (3) a *Filter* clause that contains either 1 or 2 equality conditions, specified over randomly selected categorical attributes and values from their corresponding domains; and (4) an *Analysis* clause that computes 5 aggregate functions over a numeric attribute, i.e., min, max, std, variance, and mean.

TAXI Real Dataset. The TAXI dataset is a CSV file, containing information regarding taxi rides in NYC.[8] Each record corresponds to a trip, described by 18 *attributes*. From these attributes, 5 are categorical: Payment Type, Passenger Count, Rate Type, Provider Code and Store & Forward Flag. We selected a subset of this dataset for 2014 trips with 165M objects and 26 GB CSV file size.

The Longitude and Latitude of the pick-up location are the *axis attributes* of the exploration. The *Select* clause is defined over an area of 2km × 2km size, with the *first query* Q_0 posed in central Manhattan. The *Group-by* clause contains the Passenger Count attribute, and the *Analysis* clause the Tip Amount.

NET Real Dataset. The second *real dataset* (NET) is an anonymized proprietary *telecommunication quality network dataset* containing latency and signal strength measurements crowdsourced from mobile devices in the Greater Tokyo Area (40M objects, 45GB csv file). Each record is described by 150 *attributes*. We selected the *categorical attributes*: Network Type (e.g., 4G), Network Operator Name, Device Manufacturer, Location Provider, *OS version*, and Success Flag.

The Latitude and Longitude are the *axis attributes*, simulating a map-based exploration scenario, starting from central Tokyo. The *Select* clause is defined over a 4km × 4km

[7] The data generator and the queries are available at: github.com/VisualFacts/RawVis

[8] www1.nyc.gov/site/tlc/about/tlc-trip-record-data.page

Table 3: Basic Parameters

Description	Values
Synthetic Datasets	
Number of Objects (Millions)	5, 10, 50, **100M**, 200, 500
Number of Categorical Attributes	3, 4, **6**, 10, 15
Categorical Attribute Domain Size	5 **10**, 20, 50
Synthetic & Real Datasets	
Budget Size (GB)	0.5, 1, **2**, 3, 5
Number of Bins	50, **100**, 500, 1000

area. The *Group-by* clause contains the Network Type, and Latency is used in the *Analysis* clause.

SYNTH10 / 50 Synthetic Datasets. Regarding the *synthetic datasets* (SYNTH10 / 50), we have generated two CSV files of 100M *data objects* (in the default setting), having 10 and 50 *attributes* (11 and 51 GB, respectively). The datasets contain *numeric attributes* in the range [0, 1000], as well as *categorical attributes*, where the values of the numeric and categorical attributes follow a uniform distribution. In our experiments, we vary the *number of objects* from 1M to 500M, objects with 100M being the default value, where the size of the dataset having 500M objects is 52GB. Regarding queries, as in [7], the *Select* clause is defined over two numeric attributes that specify a window size containing approximately 100K objects.

Exploration Scenario. In our evaluation, we consider a typical exploration scenario such as the one described in the introduction (Sect. 1). We have generated sequences of 100 overlapping queries, with each window query shifted (i.e., pan operation) in relation to its previous one by 10% towards a random direction. This scenario attempts to formulate a common user behavior in 2D visual exploration, where the user explores nearby regions using pan and zoom operations [49,23,43,3,47,11], such as the "region-of-interest" or "following-a-path" scenarios which are commonly used in map-based visual exploration.

Additionally, to formulate the "repetitive calculation of statistics" that commonly appears in exploration scenarios (Sect. 6.1) [46], we included the attributes of the initial query in the generated sequence of queries four times more frequently than the other dataset attributes.

VETI Parameters. Regarding VETI's tile structure, we adopt the setting used in [7], where the tile structure is initialized with 100×100 equal-width tiles, while an extra 20% of the number $|\mathcal{T}_0|$ of initial tiles was also distributed around the first query Q_0 using the Query-driven initialization method [7]. Also, the numeric threshold for the adaptation of VETI was set to 200 objects. More details about these parameters can be found at [7].

The index initialization budget, is varied from 0.5 to 5GB, with 2GB being the default value. Recall that this memory budget includes only the memory allocated by the tile and tree structures, and does not include the memory required to store the object entries.

VETI Variations. We evaluate two versions of VETI, named VETI-GRD and VETI-BINN, based on the GRD and BINN algorithms (Sect.7). Moreover, we consider a naive assignment approach, titled VETI-RND, which follows a random tile-tree assignment strategy. It first sorts the tiles based on the tile probability ρ_t, then assigns a randomly selected tree from the entire powerset $HP_{\mathcal{C}}$ to each tile, until the budget constraint $\mathcal{B}$ is satisfied.

Competitors. We compare our method with: (1) VALINOR [7] which contains only the tile-based indexing structure without the CET index; (2) A traditional DBMS (MySQL 8.0.22), where data is loaded and indexed in advance; three indexing settings are considered: (a) no indexing (SQL-0I); (b) one composite B-tree on the two axis attributes (SQL-1I); and (c) two single B-trees, one for each of the two axis attributes (SQL-2I). MySQL also supports SQL querying over external files (see CSV Storage Engine in Sect. 9); however, due to low performance [2], we do not consider it as a competitor. (3) PostgresRaw (PRAW)[9], built on top of Postgres 9.0.0 [2], which is a generic platform for in-situ querying over raw data (Sect. 9). Note that, due to parsing/processing problems on the NET dataset with the PRAW, we did not manage to load and report experiments on this combination.

Metrics. In our experiments, we measure the: (1) *Evaluation Time* of a query; (2) *Initialization Time*, which corresponds to the time required to initialize the index and return the results of the first query Q_0, i.e., from-raw data-to-1st result time. Regarding the initialization phase of the examined systems we have: (a) before evaluating Q_0, MySQL needs to parse the raw file, load, and index (except SQL-0I) the data; (b) during evaluating Q_0, PRAW needs to parse the raw file and construct the positional map; (c) during evaluating Q_0, VALINOR parses the raw file, generates the tile index structure, and populates it with the object entries; and (d) during evaluating Q_0, beyond the actions performed by VALINOR, VETI also parses the categorical attributes and constructs the tree indexes over the tiles. (3) *Overall Execution Time* of an exploration scenario, that includes: initialization time and query evaluation time for all the queries included in the exploration scenario, i.e., workload; (4) *I/O Operations* performed during query evaluation (for I/O definition see Sect. 4.3); and (5) *Index Utility*. Table 3 summarizes the parameters that we vary in the experiments.

Implementation. VETI is implemented on JVM 1.8 as part of the RawVis *open source data visualization system* [29].[2] The experiments were conducted on an 3.60GHz Intel Core i7-3820 with 64GB of RAM. We applied memory constraints (32GB max Java heap size) in order to measure the performance of our approach and our competitors. However, PRAW required more than 32GB of memory for the synthetic datasets and more than 50GB for the TAXI dataset.

[9] https://github.com/HBPMedical/PostgresRAW

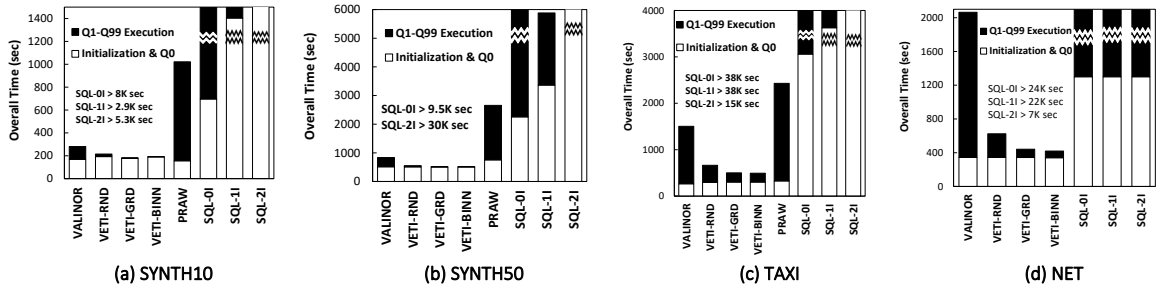

Fig. 6: Overall Time (Broken down to Initialization & $Q_1 \sim Q_{99}$ Evaluation Time)

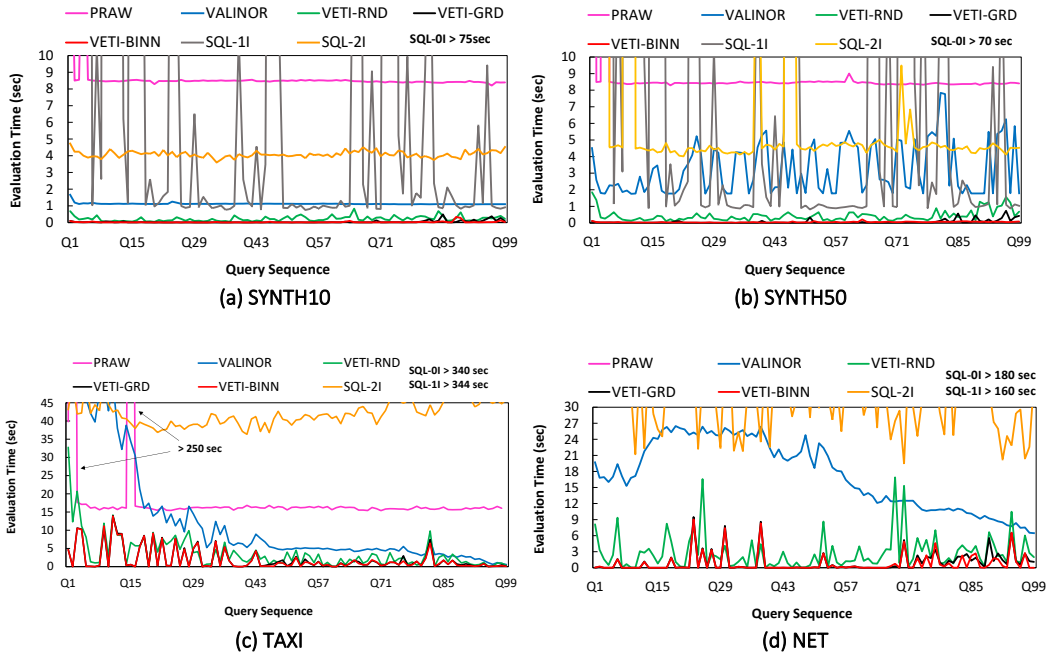

Fig. 7: Evaluation Time per Query (sec)

8.2 Performance

Initialization Phase: From-Raw Data-to-1st Result Time. Figure 6 presents the overall execution time which is split between the initialization time and the time for evaluating all the queries $Q_1 \sim Q_{99}$. Recall that, the initialization time includes the time for parsing, loading the data (in the case of MySQL), constructing the index and answering the first query Q_0. In Figure 6 we can observe that the MySQL settings we examined exhibit the worst performance for evaluating Q_0, since MySQL needs to parse all attributes of the raw file and load the data in the disk. Also, for the SQL-1I and SQL-2I cases, the corresponding indexes must be built, which explains the increased initialization time in relation to SQL-0I where no index is generated. Both VALINOR and the VETI variations exhibit better initialization performance compared to PRAW for the SYNTH50 and TAXI datasets, while for the SYNTH10 dataset, VETI requires a slightly higher initialization time. As it is expected, VETI variations are slightly slower during the initialization compared to VALINOR, since VETI needs to determine the tile-tree assignments, parse the categorical attributes, and create the tree structures. All VETI variations, however, exhibit similar initialization time, since the tile-tree assignment time is negligible compared to the time for parsing the file.

Evaluation Time per Query. Figure 7 presents the evaluation time for each individual query. Compared to the other methods, all VETI variations exhibit significantly lower evaluation time in almost all queries and datasets. In most queries, VETI reports *evaluation time less than* 0.04sec. On the other hand, the best competitors, PRAW and VALINOR require for most queries more than 8 and 4sec, respectively. Overall, VETI *is more than 200× and 100× faster compared to* PRAWand VALINOR, respectively.

Regarding SQL, SQL-0I performs worse than the 3 SQL settings we examined, and requires approximately the same time for each query. This is expected as SQL-0I has no index. From the other 2 settings, SQL-1I is for most queries faster than SQL-2I for the two synthetic datasets, and slower for TAXI and NET.

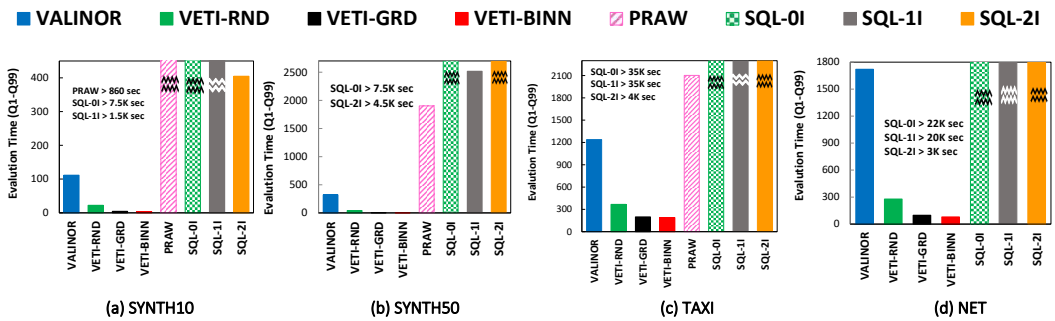

Fig. 8: Evaluation Time for $Q_1 \sim Q_{99}$ (sec)

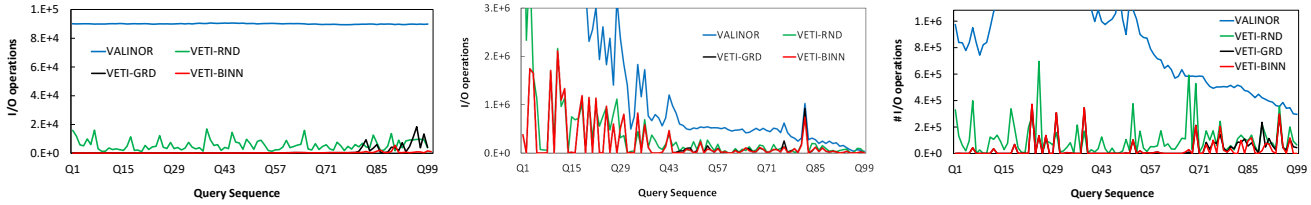

Fig. 9: Number of I/Os per Query

Regarding PRAW, we observe that it exhibits a stable performance (after the first queries), which is however worse than both VALINOR and VETI in all datasets. The positional map used in PRAW, attempts to reduce the parsing and tokenizing costs of future queries, by maintaining the position of specific attributes for every object in the raw file. However, PRAW still needs to examine all objects in the dataset in order to select the ones contained in a 2D window query. Also, in contrast to VETI, PRAW does not keep any metadata in order to efficiently compute the aggregate queries. Some of the early queries (approximately until Q_{15}) PRAW exhibits noticeably higher time than the rest, and comparable to the time required to answer Q_0. This is due to the filter conditions of the queries. When a query refers to an attribute that was not included in Q_0, PRAW needs to populate the positional map with it. In subsequent queries, which refer to indexed attributes, PRAW exhibits a relatively constant evaluation time.

Regarding VALINOR, all variations of VETI report smaller evaluation time. Even though both VALINOR and VETI attempt to adapt to the workload and maintain metadata to speed up query evaluation time by reducing I/Os, VALINOR does not include any indexing capabilities for categorical attributes and thus it needs to access the file in order to evaluate queries with conditions to such attributes. In contrast, VETI variations exploit the tree organization for evaluating filter conditions on categorical attributes and the metadata stored in the leaves for evaluating the analysis and grouping operations of queries overlapping with fully contained tiles.

Evaluation Time for all $Q_1 \sim Q_{99}$ Queries. Figure 8 presents the evaluation time for the $Q_1 \sim Q_{99}$ queries. The behavior of the methods is similarly between the datasets, the variations of VETI significantly outperform the competitors. The best competitor, VALINOR needs about 30, 60, 7 and 20× more time for SYNTH10, SYNTH50, TAXI and NET, respectively, to evaluate all queries. Also, PRAW is 270, 380 and 11× slower for SYNTH10/50 and TAXI, respectively.

I/O Operations. The evaluation time for VETI and VALINOR is mainly determined by the number of I/O operations. This can be observed in Figure 9, where the number of I/O operations per query exhibits approximately the same behavior with that of the evaluation time (Fig. 7). Note that we do not present the I/Os for PRAW and SQL, since they follow different workflows/methods for accessing the file, compared to our work. Also, the plot for SYNTH50 is omitted since it closely matches that for SYNTH10. Compared to VALINOR, the VETI variations perform up to 2 orders of magnitude less I/Os. This occurs since VALINOR has to access the raw file for every object contained in the 2D window query in order to retrieve the categorical attribute values required by the query.

8.3 VETI Variations

Performance & Assignments. Here, we compare the performance of the three VETI initialization variations. Overall, considering the performance of VETI variations (Fig. 7), both VETI-GRD and VETI-BINN lead to faster query responses than the naive VETI-RND, in almost all cases. Also, VETI-BINN significantly outperforms the other two in the number of I/Os (Fig. 9). Considering the time required for all queries (Fig. 8), VETI-RND is on average 3× slower than VETI-GRD and VETI-BINN. Comparing VETI-GRD and VETI-BINN, VETI-BINN is more than 1.5× faster than VETI-GRD (in some cases more than 100× faster) (Fig. 8), and performs more than 3× less I/Os.

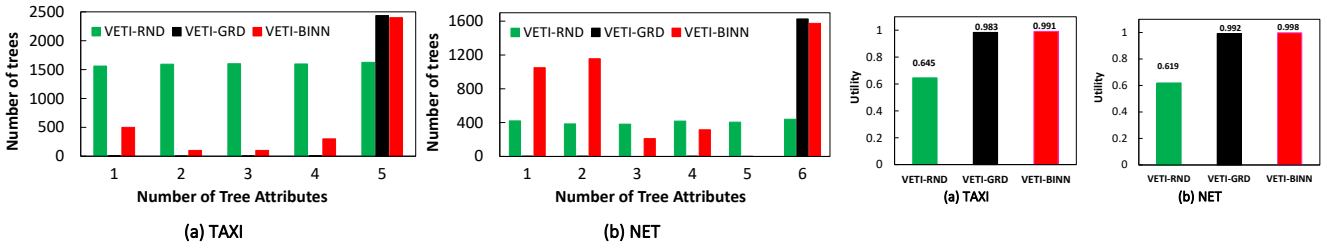

Fig. 10: Number of Generated Trees vs. Number of Tree Attributes

Fig. 11: VETI Utility Score

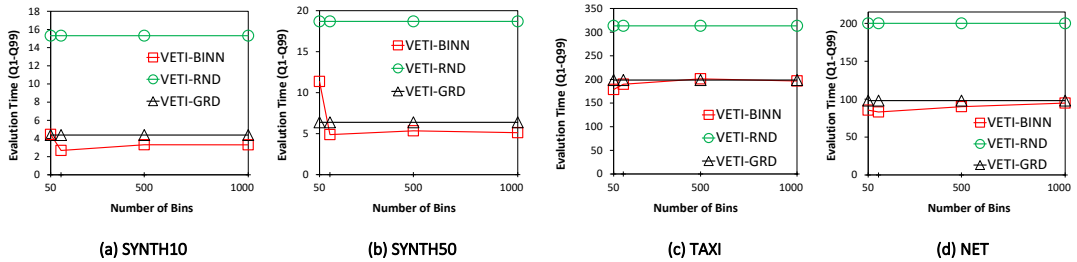

Fig. 12: VETI-BINN: Evaluation Time for $Q_1 \sim Q_{99}$ (sec) vs. Number of Bins

The difference in performance is the result of the different assignment policies (see Sect.7.3 for the policies used in VETI-BINN). Figure 10 depicts the number of trees generated during the initialization w.r.t. the number of attributes they have. For brevity, we omit the results for the synthetic datasets, as they exhibit similar behavior. We can observe, that VETI-RND follows a uniform distribution w.r.t. the number of tree attributes. In VETI-GRD the budget is mostly allocated at constructing trees that contain all of the categorical attributes. In contrast, VETI-BINN creates a more balanced distribution of the trees' number of attributes. As a result, VETI-GRD assigns "taller" trees to a smaller number of tiles. So, due to location-based assignments process we follow, the tiles located farther away from Q_0 tend to not contains trees. This is why, compared to VETI-GRD, VETI-BINN tends to perform even better when the user moves away from the initial starting point. This is demonstrated, in the query performance where, in most cases, after query Q_{75}, VETI-BINN is 10× faster than VETI-GRD in (Fig. 7); also, in some queries is up to 400× faster (Fig. 7d).

The impact of the different assignment strategies is also shown in the utility score (Fig. 11). Due to randomized tree assignments, VETI-RND results in a lower utility score, whereas VETI-BINN exhibits larger utility compared to VETI-GRD.

VETI-BINN: Varying the Number of Bins. In this experiment we study the performance of VETI-BINN w.r.t. the number of bins. Figure 12 presents the evaluation time for $Q_1 \sim Q_{99}$, varying the number of bins from 50 to 1000. Note that, in the plots we include VETI-RND and VETI-GRD for the sake of comparison, even though they do not depend on the number of bins.

As we can observe, the performance of VETI-BINN is not highly affected by the number of bins, except for small number of bins, i.e., between 50 and 100. Based on our adopted assignment policies for VETI-BINN (Sect. 7.3), the following holds. For small numbers of bins, the assignment is more coarse-grained, i.e., shorter trees are assigned to the majority of the tiles. Increasing the number of bins results in more fine-grained assignments of trees to (bins of) tiles. However, trees that are assigned to bins near Q_0 will be taller, whereas the trees assigned to the remaining bins will be short. This explains why, in general, as the number of bins increase, the performance of VETI-BINN approaches that of VETI-GRD. Recall that VETI-GRD assigns mostly tall trees (Fig. 10).

As previously mentioned, we should note that, the definition of bins depends on the dataset characteristics and the exploration scenario. As a general observation, in exploration scenarios with queries affecting areas away from the initial starting point, the number of bins should be kept relatively small in order to create trees (even short ones) to the majority of the tiles, whereas in scenarios focused on a specific area, increasing the number of bins performs better.

Varying the Initialization Memory Budget. In the first experiment, we evaluate the performance of VETI while varying the initialization budget from 0.5 to 5GB. Recall that this memory budget includes only the memory allocated by the tile and tree structures, and does not include the memory required to store the object entries. Note that, the plots for the SYNTH10/50 datasets are omitted since they are similar to the ones presented.

The evaluation time needed to evaluate all the queries is shown in Figure 13. The evaluation time decreases as the available memory budget increases. This is the result of the larger number and more detailed tree structures that are constructed with more budget, which leads to faster query evaluation. This is observed in both VETI-GRD and VETI-BINN. Regarding VETI-RND, its performance does not always im-

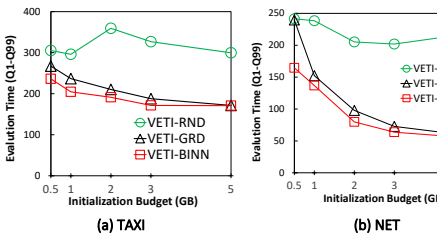

Fig. 13: Evaluation Time for $Q_1 \sim Q_{99}$ (sec) vs. Initialization Memory Budget

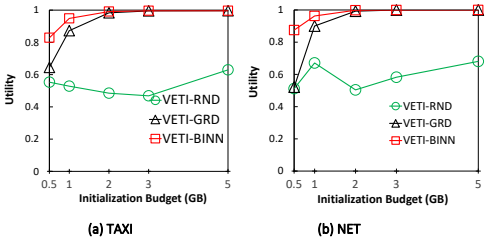

Fig. 14: VETI Utility vs. Initialization Memory Budget

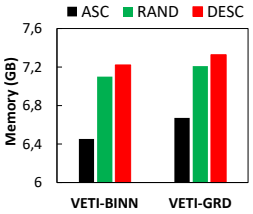

Fig. 15: Memory Size vs. Sorting Attributes based on Domain Size

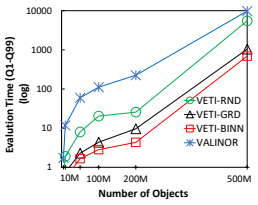

Fig. 16: Evaluation Time (log) vs. Number of Objects [SYNTH10]

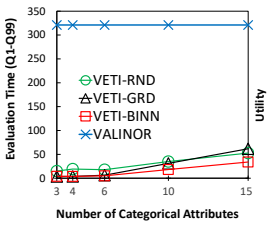

(a) Evaluation Time (sec)

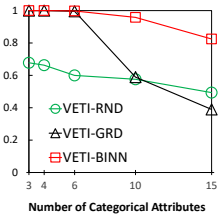

(b) Utility

Fig. 17: Varying the Number of Cat. Attributes [SYNTH50]

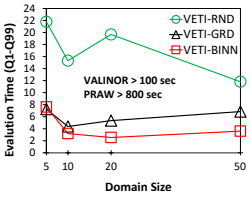

(a) Evaluation Time (sec)

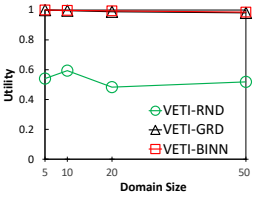

(b) Utility

Fig. 18: Varying the Domain Size of Cat. Attributes [SYNTH10]

prove when increasing the budget, as it allocates the budget in random tile-tree assignments.

Compared to VETI-GRD, VETI-BINN's performance is less dependent on the available budget. VETI-GRD performs much worse for low values of memory budget, as it mostly assigns trees with all the categorical attributes which quickly depletes the budget on very few tiles. On the other hand, as the budget increases, the performance of VETI-GRD is comparable with that of VETI-BINN.

In more details, on small amounts of budget, VETI-BINN evaluates all the queries of the exploration scenario in half the time compared to VETI-GRD (Fig. 13). Moreover, at query level, in several queries, compared to VETI-GRD, VETI-BINN is from 100 to 3000× faster for the NET dataset; and more than 50× for SYNTH10/50.

In this experiment, we compute the utility score w.r.t. memory budget. (Fig. 14). The results closely match the evaluation time presented above. Specifically, the total index utility increases with higher budget for both VETI-GRD and VETI-BINN. Also, the utility of VETI-GRD is much lower than that of VETI-BINN for smaller amounts of budget, but their values converge as the budget increases.

VETI Memory Size vs. Sorting Tree Attributes. In this experiment, we examine how the sorting of tree attributes w.r.t. their domain size affects the allocated memory (more details in Sect. 3). In order to assess the effect of domain size, we create a version of the SYNTH10 where its categorical attributes had a different domain size, varying from 2 to 100. We measured the VETI memory size after initialization while sorting the attributes based on their domain sizes in ascending (ASC), descending (DESC), and random (RAND) order. As it can be seen in Figure 15, ASC ordering corresponds to the best case, while DESC to the worst. Specifically, for VETI-BINN the ASC ordering results in a decrease in memory size of around 10% and 8% in relation to DESC and RAND, respectively. Similar results are reported for VETI-GRD.

8.4 Effect of the Data Characteristics

Varying the Number of Objects. In this experiment, we evaluate the impact of the number of objects on the performance of VETI. For this, we vary the number of objects of SYNTH10 from 5 to 500M, and the evaluation time for $Q_1 \sim Q_{99}$ is presented in Figure 16. As the total number of objects in the file increase, the evaluation time increases (sub-)linearly for all variations of VETI as well as for VALINOR. This is reasonable considering that the index becomes more dense, the queries relatively select more objects and the number of required I/O operations increase; also, the cost of an I/O operation becomes "relatively" larger when the file size increase. Regarding VETI-RND, its performance is affected to a much greater extent compared to VETI-GRD and VETI-BINN, as its randomized tree assignment lead to a much higher I/O cost.

Varying the Number of Categorical Attributes. In this experiment, we vary the number of categorical attributes (Fig. 17). Here, we used the SYNTH50 dataset in order to be able to select up to 15 categorical attributes. For brevity the SQL and PRAW methods are omitted, as they exhibit much higher evaluation time. Also, we could not evaluate PRAW for 15 categorical attributes, due to increased mem-

ory requirements. Note that VALINOR's performance is not affected by the number of categorical attributes, since it does not consider them in its index structure.

As we can observe, query evaluation time increases for all methods, along with the number of attributes (Fig. 17(a)). VETI-BINN outperforms both VETI-RND and VETI-GRD. Regarding VETI-GRD, we can observe that it outperforms VETI-RND in every case except for the case of 15 categorical attributes. This is due to the fact that VETI-GRD allocates most of the budget for creating trees with all the categorical attributes. As a result, with a higher number of categorical attributes, VETI-GRD assigns trees to very few tiles, which explains its performance deterioration for 15 attributes. This is also depicted in Figure 17(b) which presents the utility score. As we can observe, in all VETI variations the utility score decreases as the number of categorical attributes indexed increase. This decrease is even more notable in the case of VETI-GRD, which after 10 attributes gets worse than both VETI-BINN and VETI-RND.

Varying the Domain Size of Categorical Attributes. In this experiment, we study the effect of the domain size. We generate 4 different versions of the SYNTH10 dataset, where the domain size of each categorical attribute for each one was set to 5, 10, 20 and 50. Note that, the results for the SYNTH50 are not presented since they are similar.

The evaluation time needed to execute the $Q_1 \sim Q_{99}$ is shown in Figure 18(a). Note that the plot shows only the VETI variations, since VALINOR does not depend on the domain, and others exhibit much higher evaluation time. We can observe that the evaluation time of VETI-GRD (resp. VETI-BINN) decreases from domain size 5 to 10 (resp. 20), and then increases.

This behavior is explained as follows. The attributes in the synthetic dataset have values, which are uniformly distributed over the objects. As the domain size of an attribute increases, the number of objects, which evaluate to the filter condition on this attribute, decreases, and so does the number of I/O operations. This explains the initial drop in query evaluation time for both VETI-GRD and VETI-BINN.

On the other hand, given the same number of attributes, a larger domain size results in trees with larger size in memory (Sect. 3.1). This explains the increase in evaluation time after domain size 10 for VETI-GRD and 20 for VETI-BINN, as the larger tree sizes result in fewer tiles getting assigned with trees.

9 Related Work

In-situ Raw Data Processing. Data loading and indexing usually take a large part of the overall time-to-analysis for both traditional RDBMs and Big Data systems [18]. In-situ query processing aims at avoiding data loading in a DBMS by accessing and operating directly over raw data files. NoDB [2] was a first approach for a no-dbms querying engine over raw data, and PostgresRAW is one of the first systems for in-situ query processing. PostgresRAW incrementally builds on-the-fly auxiliary indexing structures called "positional maps" which store the file positions of data attributes, as well as it stores previously accessed data into cache. As opposed to VETI, the positional map in PostgresRAW, can only be exploited to reduce parsing and tokenization costs during query evaluation and can not be used to reduce the number of objects examined in two-dimensional range queries. Also, VETI is better optimized for aggregate queries, since it can reduce raw file accesses by reusing already calculated statistics on a tile level. Finally, VETI offers memory-driven index initialization, by adjusting its initial parameters w.r.t. available resources.

DiNoDB [44] is a distributed version of PostgresRAW. In the same direction, PGR [25] extends the positional maps in order to both index and query files in formats other than CSV. In the same context, Proteus [24] supports various data models and formats. Recently, Slalom [35,36] exploits the positional maps and integrates partitioning techniques that take into account user access patterns.

Raw data access methods have been also employed for the analysis of scientific data, usually stored in array-based files. In this context, Data Vaults [20] and SDS/Q [9] rely on DBMS technologies to perform analysis over scientific array-based file formats. Further, SCANRAW [10] considers parallel techniques to speed up CPU intensive processing tasks associated with raw data accesses.

[7,6] define VALINOR, a tile-based index in the context of in-situ visual exploration, supporting 2D visual operations over numeric attributes. Compared to VETI, VALINOR does not support operations and indexing over categorical attributes and does not consider memory-driven index initialization.

To note that, several well-known DBMS support SQL querying over CSV files. Particularly, MySQL provides the CSV Storage Engine[10], Oracle offers the External Tables[11] and Postgres has the Foreign Data[12] However, these tools do not focus on user interaction, parsing the entire file for each posed query, and resulting in significantly low query performance [2].

Visual-Oriented Indexes. In the context of visual exploration, several indexes have been introduced. VisTrees [12] and HETree [8] are tree-based main-memory indexes that address visual exploration use cases, i.e., they offer exploration-oriented features such as incremental index construction and adaptation. Compared to our work, both indexes focus on one-dimensional visualization techniques (e.g., histograms), do not support categorical attributes and group-by analytics, and do not consider disk storage, i.e., data stored in-memory.

Nanocubes [27], Hashedcubes [26], SmartCube [28], Gaussian Cubes [45], and TopKubes [31] are main-memory data structures defined over spatial, categorical and temporal data. The aforementioned works are based on main-memory variations of a data cube in order to reduce the time needed

[10] https://dev.mysql.com/doc/refman/8.0/en/csv-storage-engine.html

[11] https://oracle-base.com/articles/12c/external-table-enhancements-12cr1

[12] www.postgresql.org/docs/current/ddl-foreign-data.html

to generate visualizations. Nanocubes [27] attempts to reduce the memory of the data cube by sharing nodes in a single tree structure. Hashedcubes [26] follows a different approach where, instead of materializing all possible aggregations, it uses a partial ordering of the dimensions and the notion of pivot arrays to calculate on-the-fly the aggregations missing. Smartcube [28] is a variation of Nanocubes, where instead of pre-computing all cuboids from the start, it chooses some important ones based on the user queries, in order to reduce memory usage. Also, it may adaptively change stored cuboids when querying patterns change. In comparison with our work, the indexes in the aforementioned works are generated during a preprocessing phase, and thus cannot be used in in-situ scenarios, e.g., they do not address problems related to reducing the initialization time. Moreover, a major difference compared to our approach, is that these works assume that all the aggregations are materialized and stored in main memory, which in most cases require prohibitive amounts of memory. In contrast, our approach considers limited memory resources.

Further, graphVizdb [5,4] is a graph-based visualization tool, which employs a 2D spatial index (e.g., R-tree) and maps user interactions to 2D window queries. To support the operation of the tool, a partition-based graph drawing approach is proposed. Spatial 2D indexing is also adopted in Kyrix [42]. Kyrix is a generic platform that supports efficient Zoom and Pan operations over arbitrary data types. Initially, the data is stored in a database and indexed using R-trees. In both graphVizdb and Kyrix the zoom levels are predefined, with each level having its own table and R-tree. Each Pan and Zoom operation is mapped to a rectangle 2D query, and based on the zoom level, is evaluated over the corresponding table and R-tree.

Compared to our work, the aforementioned systems require a preprocessing phase where data is first stored and indexed in a database system. On the other hand, our work is defined in an in-situ setting, over limited memory resources. To improve query evaluation performance and reduce the I/O costs, our work is based on in-memory incremental and adaptive indexing and query evaluation methods. On the other hand, in Kyrix, queries are evaluated over fixed database indexes, while a caching and prefetching strategy is used to reduce the database access cost. Another difference is related to the evaluation of statistics. Our work focuses on efficient statistics computations by utilizing stored metadata to reduce the required I/O operations. On the other hand, the aforementioned works do not study the problem of efficient statistics computations.

In a different context, tile-based structures are used in visual exploration scenarios. Semantic Windows [23] considers the problem of finding rectangular regions (i.e., tiles) with specific aggregate properties in exploration scenarios. ForeCache [3] considers a client-server architecture in which the user visually explores data from a DBMS. The approach proposes a middle layer, which prefetches tiles of data based on user interaction. Our work considers different problems compared to the aforementioned approaches.

Adaptive Indexing. Similarly to VETI, the basic idea of approaches like database cracking and adaptive indexing is to incrementally adapt the indexes and/or refine the physical order of data, during query processing, following the characteristics of the workload [21,16,48,19,34,16,17,33,38].

However, these works are not designed for the in-situ scenario. In most cases the data has to be previously loaded / indexed in the system/memory, i.e., a preprocessing phase is considered. Additionally, the aforementioned works refine the (physical) order of data, performing highly expensive data duplication and allocate large amount of memory resources. Nevertheless, in the *in-situ scenarios* the analysis is performed directly over immutable raw data files considering limited resources.

Furthermore, most of the existing cracking and adaptive indexing methods have been developed in the context of column-stores or MapReduce systems [41]. On the other hand, VETI has been developed to handle raw data stored in text files with commodity hardware.

Progressive Visualization. Recently, many systems adopt the progressive paradigm attempting to reduce the response time [13,40,1,14]. Progressive approaches, instead of performing all the computations in one step (that can take a long time to complete), splits them in a series of short chunks of approximate computations that improve with time. Compared to these works, we do not consider progressive and approximate computations; rather exact answers are presented to the users as soon as they are computed.

10 Conclusions

In this paper, we presented our work that enables efficient in-situ visual exploration and analysis of data visualized in a 2D plane. The indexing scheme and adaptive processing methods we described allow the visual exploration of data from a raw file on a 2D visual representation, along with sophisticated analysis over its numeric, spatial, and categorical attributes. This scheme is constructed on-the-fly given the first user query, and is progressively adapted based on user interactions. To handle the large memory requirements, we formulated the index initialization as an optimization problem and provided two approximate algorithms for its solution. Further, we presented efficient query evaluation methods that achieve fast user response by reusing available metadata stored in the index, avoiding I/O operations. Finally, we conducted a thorough experimental evaluation which demonstrates that the proposed methods significantly outperform existing solutions.

Acknowledgment. This work has been funded by the project VisualFacts (#1614 - 1st Call of the Hellenic Foundation for Research and Innovation Research Projects for the support of post-doctoral researchers).

References

1. Agarwal, S., Mozafari, B., Panda, A., Milner, H., Madden, S., Stoica, I.: Blinkdb: Queries with Bounded Errors and Bounded Response Times on Very Large Data. In: European Conference on Computer Systems (EuroSys) (2013)
2. Alagiannis, I., Borovica, R., Branco, M., Idreos, S., Ailamaki, A.: Nodb: Efficient Query Execution on Raw Data Files. In: ACM Conf on Management of Data (SIGMOD) (2012)
3. Battle, L., Chang, R., Stonebraker, M.: Dynamic Prefetching of Data Tiles for Interactive Visualization. In: ACM Conf on Management of Data (SIGMOD) (2016)
4. Bikakis, N., Liagouris, J., Krommyda, M., Papastefanatos, G., Sellis, T.: Towards Scalable Visual Exploration of Very Large Rdf Graphs. In: Extended Semantic Web Conference (ESWC) (2015)
5. Bikakis, N., Liagouris, J., Krommyda, M., Papastefanatos, G., Sellis, T.: Graphvizdb: A Scalable Platform for Interactive Large Graph Visualization. In: IEEE ICDE (2016)
6. Bikakis, N., Maroulis, S., Papastefanatos, G., Vassiliadis, P.: RawVis: Visual Exploration over Raw Data. In: Advances in Databases and Information Systems (ADBIS) (2018)
7. Bikakis, N., Maroulis, S., Papastefanatos, G., Vassiliadis, P.: In-situ Visual Exploration over Big Raw Data. Inform. Sys. **40** (2021)
8. Bikakis, N., Papastefanatos, G., Skourla, M., Sellis, T.: A Hierarchical Aggregation Framework for Efficient Multilevel Visual Exploration and Analysis. Semantic Web Journal (2017)
9. Blanas, S., Wu, K., Byna, S., Dong, B., Shoshani, A.: Parallel Data Analysis Directly on Scientific File Formats. In: ACM Conf on Management of Data (SIGMOD) (2014)
10. Cheng, Y., Rusu, F.: SCANRAW: a Database Meta-operator for Parallel In-situ Processing and Loading. ACM TODS **40**(3) (2015)
11. Dar, S., Franklin, M.J., THór Jónsson, B., Srivastava, D., Tan, M.: Semantic Data Caching and Replacement. In: (VLDB) (1996)
12. El-Hindi, M., Zhao, Z., Binnig, C., Kraska, T.: Vistrees: Fast Indexes for Interactive Data Exploration. In: HILDA (2016)
13. Fekete, J., Fisher, D., Nandi, A., Sedlmair, M.: Progressive Data Analysis and Visualization (Dagstuhl Seminar 18411). Dagstuhl Reports **8**(10) (2018)
14. Fisher, D., Popov, I.O., Drucker, S.M., Schraefel, M.C.: Trust Me, I'm Partially Right: Incremental Visualization Lets Analysts Explore Large Datasets Faster. In: CHI (2012)
15. Gray, J., Chaudhuri, S., Bosworth, A., Layman, A., Reichart, D., Venkatrao, M., Pellow, F., Pirahesh, H.: Data Cube: A Relational Aggregation Operator Generalizing Group-by, Cross-Tab, and Sub Totals. Data Min. Knowl. Discov. **1**(1) (1997)
16. Holanda, P., Manegold, S.: Progressive mergesort: Merging batches of appends into progressive indexes. In: Conf on Extending Database Technology (EDBT) (2021)
17. Holanda, P., Manegold, S., Mühleisen, H., Raasveldt, M.: Progressive Indexes: Indexing for Interactive Data Analysis. PVLDB Endowment **12**(13) (2019)
18. Idreos, S., Alagiannis, I., Johnson, R., Ailamaki, A.: Here Are My Data Files. Here Are My Queries. Where Are My Results? In: Conf on Innovative Data Systems Research (CIDR) (2011)
19. Idreos, S., Kersten, M.L., Manegold, S.: Database Cracking. In: Conf on Innovative Data Systems Research (CIDR) (2007)
20. Ivanova, M., Kersten, M.L., Manegold, S., Kargin, Y.: Data Vaults: Database Technology for Scientific File Repositories. Computing in Science and Engineering **15**(3) (2013)
21. Jensen, A.H., Lauridsen, F., Zardbani, F., Idreos, S., Karras, P.: Revisiting multidimensional adaptive indexing [experiment & analysis]. In: Conf on Extending Database Technology (EDBT) (2021)
22. Jugel, U., Jerzak, Z., Hackenbroich, G., Markl, V.: VDDa: Automatic Visualization-driven Data Aggregation in Relational Databases. Journal on Very Large Data Bases (VLDBJ) (2015)
23. Kalinin, A., Çetintemel, U., Zdonik, S.B.: Interactive Data Exploration Using Semantic Windows. In: ACM SIGMOD (2014)
24. Karpathiotakis, M., Alagiannis, I., Ailamaki, A.: Fast Queries Over Heterogeneous Data Through Engine Customization. PVLDB **9**(12) (2016)
25. Karpathiotakis, M., Branco, M., Alagiannis, I., Ailamaki, A.: Adaptive Query Processing on Raw Data. PVLDB **7**(12) (2014)
26. de Lara Pahins, C.A., Stephens, S.A., Scheidegger, C., Comba, J.L.D.: Hashedcubes: Simple, Low Memory, Real-time Visual Exploration of Big Data. IEEE Trans on Visualization & Computer Graphics **23**(1) (2017)
27. Lins, L.D., Klosowski, J.T., Scheidegger, C.E.: Nanocubes for Real-Time Exploration of Spatiotemporal Datasets. IEEE Trans on Visualization & Computer Graphics **19**, 2456–2465 (2013)
28. Liu, C., Wu, C., Shao, H., Yuan, X.: Smartcube: An adaptive data management architecture for the real-time visualization of spatiotemporal datasets. IEEE TVCG **26**(1) (2020)
29. Maroulis, S., Bikakis, N., Papastefanatos, G., Vassiliadis, P.: RawVis: A System for Efficient In-situ Visual Analytics. In: ACM Conf on Management of Data (SIGMOD) (2021)
30. Maroulis, S., Bikakis, N., Papastefanatos, G., Vassiliadis, P., Vassiliou, Y.: Adaptive indexing for in-situ visual exploration and analytics. In:DOLAP Workshop (2021)
31. Miranda, F., Lins, L., Klosowski, J.T., Silva, C.T.: TopKube: A Rank-Aware Data Cube for Real-Time Exploration of Spatiotemporal Data. IEEE TVCG **24**, (2017)
32. Morton, K., Balazinska, M., Grossman, D., Mackinlay, J.D.: Support the Data Enthusiast: Challenges for Next-generation Data-analysis Systems. VLDB Endowment **7**(6) (2014)
33. Nathan, V., Ding, J., Alizadeh, M., Kraska, T.: Learning multi-dimensional indexes. In: ACM SIGMOD (2020)
34. Nerone, M., Holanda, P., de Almeida, E.C., Manegold, S.: Multi-dimensional Adaptive and Progressive Indexes. In: IEEE Conf on Data Engineering (ICDE) (2021)
35. Olma, M., Karpathiotakis, M., Alagiannis, I., Athanassoulis, M., Ailamaki, A.: Slalom: Coasting through Raw Data Via Adaptive Partitioning and Indexing. VLDB Endowment **10**(10) (2017)
36. Olma, M., Karpathiotakis, M., Alagiannis, I., Athanassoulis, M., Ailamaki, A.: Adaptive partitioning and indexing for in situ query processing. Journal on Very Large Data Bases (VLDBJ) (2019)
37. Papastefanatos, G., Alexiou, G., Bikakis, N., Maroulis, S., Stamatopoulos, V.: Visualfacts: A platform for in-situ visual exploration and real-time entity resolution. In: Workshop on Big Data Visual Exploration & Analytics (BigVis) (2022)
38. Pavlovic, M., Sidlauskas, D., Heinis, T., Ailamaki, A.: QUASII: query-aware spatial incremental index. In: Conf on Extending Database Technology (EDBT) (2018)
39. Rahman, P., Jiang, L., Nandi, A.: Evaluating Interactive Data Systems. Journal on Very Large Data Bases (VLDBJ) **29**(1) (2020)
40. Rahman, S., Aliakbarpour, M., Kong, H., Blais, E., Karahalios, K., Parameswaran, A.G., Rubinfeld, R.: I've Seen "Enough": Incrementally Improving Visualizations to Support Rapid Decision Making. VLDB Endowment **10**(11) (2017)
41. Richter, S., Quiané-Ruiz, J., Schuh, S., Dittrich, J.: Towards zero-overhead static and adaptive indexing in Hadoop. Journal on Very Large Data Bases (VLDBJ) **23**(3) (2014)
42. Tao, W., Liu, X., Wang, Y., Battle, L., Demiralp, Ç., Chang, R., Stonebraker, M.: Kyrix: Interactive pan/zoom visualizations at scale. Comput. Graph. Forum **38**(3) (2019)
43. Tauheed, F., Heinis, T., Schürmann, F., Markram, H., Ailamaki, A.: SCOUT: Prefetching for Latent Feature Following Queries. VLDB Endowment **5**(11) (2012)
44. Tian, Y., Alagiannis, I., Liarou, E., Ailamaki, A., Michiardi, P., Vukolic, M.: Dinodb: An Interactive-speed Query Engine for Ad-hoc Queries on Temporary Data. IEEE Trans. on Big Data (2017)
45. Wang, Z., Ferreira, N., Wei, Y., Bhaskar, A.S., Scheidegger, C.: Gaussian cubes: Real-time modeling for visual exploration of large multidimensional datasets. IEEE Trans on Visualization & Computer Graphics **23**(1) (2017)
46. Wasay, A., Wei, X., Dayan, N., Idreos, S.: Data Canopy: Accelerating Exploratory Statistical Analysis. In: ACM SIGMOD (2017)
47. Yesilmurat, S., Isler, V.: Retrospective adaptive prefetching for interactive Web GIS applications. GeoInformatica **16**(3) (2012)
48. Zardbani, F., Afshani, P., Karras, P.: Revisiting the theory and practice of database cracking. In: EDBT (2020)
49. Zhao, W., Rusu, F., Dong, B., Wu, K., Ho, A.Y.Q., Nugent, P.: Distributed caching for processing raw arrays. In: Conf on Scientific & Statistical Database Management (SSDBM) (2018)